Research Square

Preprints are preliminary reports that have not undergone peer review.
They should not be considered conclusive, used to inform clinical practice,
or referenced by the media as validated information.

Fc and tailpiece determinants of IgM tailpiece-mediated IgG hexamerisation

Shirley Peters

shirley.peters@ucb.com

UCB Pharma

Joshua Sopp

Joshua Ede

Zainab Ahdash

Hanna Hailu

UCB Pharma (United Kingdom)

Adam Hold

Ben Holmes

Mark Cragg

University of Southampton

David Humphreys

UCB https://orcid.org/0009-0004-6487-3406

Article

Keywords: Fc engineering, hexamerisation, IgM tailpiece, isotype, R355, CDC

Posted Date: August 8th, 2026

DOI: https://doi.org/10.21203/rs.3.rs-10432191/v1

License: This work is licensed under a Creative Commons Attribution 4.0 International License.
Read Full License

Additional Declarations: There is **NO** Competing Interest.

Fc and tailpiece determinants of IgM tailpiece-mediated IgG hexamerisation

Shirley J. Peters[1], Joshua M. Sopp[2], Joshua Ede[1], Zainab Ahdash[1], Hanna Hailu[1], Adam Hold[1], Ben Holmes[1], Mark S. Cragg[2], David P. Humphreys[1]

[1]UCB, Slough, UK. [2]Antibody and Vaccine Group, Centre for Cancer Immunology, Cancer Sciences, Faculty of Medicine, University of Southampton, Southampton, UK.

Corresponding author: Shirley J. Peters: Shirley.peters@ucb.com

Abstract (<150 words):

The IgM tailpiece (μtp) promotes hexamerisation and covalent stabilisation of Fc and IgG. We used IgG Fc-tailpiece fusions to define how Fc and tailpiece features contribute to hexamer formation. Efficient tp-driven hexamerisation required Cγ3 domain residues, tailpiece amino acids, N-linked glycans in both Cγ2 and μtp, and interchain disulphide bonds. R355 in the Cγ3 domain emerged as a key determinant: IgG4, hexamerised poorly, whereas Q355R restored hexamerisation. Tailpiece mutagenesis identified variants that enhanced or disrupted non-covalent hexamer formation, including S565T, which improved hexamerisation and CDC activity. Overall, these data reveal coordinated Fc-tailpiece determinants of IgG hexamerisation and support engineering multimeric therapeutic antibodies with enhanced functional activity.

Key words: Fc engineering, hexamerisation, IgM tailpiece, isotype, R355, CDC

Abbreviations: tailpiece (tp), IgM tailpiece (μtp), IgA tailpiece (αtp), disulphide bond (DSB), full-length (FL), intravenous immunoglobulin (IVIg), Rituximab (RTX), Complement dependent cytotoxicity (CDC)

Introduction

The therapeutic application of IgG-based monoclonal antibodies continues to expand, driven by advances in antibody engineering aimed at optimizing clinical performance[1,2]. Current strategies include afucosylation to enhance antibody-dependent cellular cytotoxicity (ADCC), Fc domain modifications to fine-tune Fcγ receptor (FcγR) interactions and prolong serum half-life[2-4], and approaches that augment agonistic signalling. In addition, the design of multimeric Fc constructs and multivalent IgG formats—achieved through fusion to IgM tailpieces or alternative Fc engineering approaches—has emerged as a promising strategy for improving therapeutic efficacy, particularly where increased avidity, complement activation or receptor clustering is desired[2,5-9].

Immunoglobulins are classified into four major isotypes: IgA, IgE, IgG, and IgM. Among these, IgM exists naturally either as a pentamer, when associated with J-chain, or hexamer, with multimerisation predominantly driven by the presence of a carboxy-terminal tailpiece (tp)[10-12]. The human IgM-tp (μtp) is an 18 amino acid peptide ($PTLYN_{563}VSLVMSDTAGTC_{575}Y$) that contains two key features, an N-linked glycosylation site (N563) and a penultimate cysteine (C575) – both are key to effective multimerisation[11,13,14]. Additionally, two Cys residues, located at positions 337 (Cμ2) and 414 (Cμ3), along with non-covalent interactions throughout the Fc and tailpiece regions, further stabilise IgM multimerisation[15-17]. Key tp residues essential for IgM multimerisation were previously identified [18] and further elucidated when the structure of pentameric IgM was reported[19]. These data confirm formation of an inter-tp disulphide bond (DSB) between two neighbouring C575 residues. The structure further revealed β-strands from Tyr562 to Met568 arranged as 2 × 5 parallel β-sheets with Tyr562, Val564, Leu566 and Met568 forming essential hydrophobic interactions that stabilise hexamer formation[19].

IgM is typically present with low affinity Fab arms and as such requires multimerisation to increase functional avidity and ensure effective target antigen engagement. IgM directly combats microbial infections *via* complement-mediated effector functions[20,21]. A single multimeric IgM molecule, if bound to antigen, can interact with C1q to initiate the classical complement pathway[22], resulting in the deposition of C3 fragments, release of anaphylatoxins and cell lysis. Pentameric IgM $(\mu_2L_2)_5J$ is formed in the presence of the J chain and makes up the greatest fraction of circulating IgM. Hexameric IgM $(\mu_2L_2)_6$, is the more potent complement activator and previous work established the J-chain substitutes structurally for the sixth Cμ4 domain in the pentameric form[3,6,7].

Certain IgG subclasses can also activate the classical complement pathway, most notably when they arrange into non-covalent hexamers which can then interact with the six C1q binding subunits of C1 to initiate complement activation in a similar manner to IgM[9,23]. In order to combine hexameric IgM's potent complement activation and IgG's FcγR engagement capabilities, IgG3-μtp fusions carrying a L309C mutation (which corresponds to Cys414 of IgM) were previously generated, resulting in polymeric IgG estimated to be disulphide-bonded pentamer and/or hexamer[24]. Subsequently, multimeric IgGs have been generated in each of the four human IgG isotypes, with the conventionally complement inactive IgG2 and IgG4 isotypes demonstrating enhanced complement-dependent cytotoxicity (CDC) and cell lysis[8,25].

Hexameric forms of Fc have also been created using IgM tailpiece fusions[7,8,26-28]. These engineered molecules increase binding to the low-affinity FcγRs and / or C1q in an avidity driven manner, blocking or sequestering them at much lower concentrations compared to intravenous immunoglobulin (IVIg). Qureshi et al. described differential hexamer formation between IgG1 Fc-μtp and IgG4 Fc-μtp fusions when produced from CHO-SXE cells. IgG Fc-μtp fusion molecules readily formed Fc-hexamers whereas IgG4 hexamer formation was much less efficient[7].

We were interested to understand the fundamental processes behind this difference and the contribution of both the Fc and tp residues to hexamerisation. We explored this by testing mutations within the human Cγ3 domain and μtp using a panel of human IgG1 Fc and IgG4 Fc mutants and hybrids thereof fused to μtp and μtp variants. We confirmed the importance of N-linked glycosylation in both Cγ2 domains and tp, and hydrophobic residues L561, Y562, L566, V567 and M568 within the tp for structural stability and efficient hexamer formation. We further identified R355 in the IgG Cγ3 domain as a key residue which was critical in Fc hexamer formation efficiency for both IgG1 and IgG4 Fc. Additionally, it has also been reported that the sequence of the N-linked glycan motif (N-X-S/T) can contribute to the efficiency of glycosylation[29], hence we explored different amino acid residues at positions 564 and 565 and identified the S565T variant as promoting hexamerisation. By introducing the hexamer-enhancing variants Q355R and S565T into the IgG1-μtp$_{C575S}$ or IgG4P-μtp$_{C575S}$ fusion molecules, we observed an improved hexamer formation in solution, which was accompanied by a corresponding enhancement in CDC activity.

Material and Methods

Construct design and generation:

The EU numbering system was used for all amino acid number allocations. In the case of tp fusion proteins, numbers for the tp were retained as per the EU numbering system and not renumbered.

Fc-tp constructs were designed to contain the core hinge ($C_{226}P_{227}P_{228}C_{229}$) of an IgG fused to the IgG Cγ2 domain (with or without L309C) and the Cγ3 domain with an IgM or IgA tailpiece at the C-terminus (Figures 1A and B). Human IgGs were each directly fused at their C-terminal lysine residues to the wild-type 18 amino acid (PTLYNVSLVMSDTAGTCY) tp as described previously[8]. Fc-tp and IgG-µtp DNA constructs were ordered from ATUM. Point mutations were introduced to DNA either by ordering the full gene from ATUM or by performing site directed mutagenesis using Agilent's QuikChange lightning kits (Agilent) according to manufacturer's instructions. Oligonucleotides were designed using Agilent's web primer design tool.

Protein production

DNA constructs were expressed in UCB's proprietary CHO-SXE cell line [30], using the ExpiCHO transfection system following the high yield protocol (Thermo Fisher Scientific). Following centrifugation of cell cultures for 1 hour at 4000 × g, supernatants were clarified using 0.22 µm Stericup filters (Millipore). Secreted product concentration was determined by loading 100 µl of culture supernatant onto a Poros G column (Thermo Fisher Scientific) attached to an Infinity high-performance liquid chromatography (HPLC) system (Agilent). Product was eluted off the column with 0.1 M NaCl, pH 2.1 and the A_{280} signal was compared to a purified Fab standard. Clarified supernatant was loaded onto a 10 ml MabSelect SuRe column (Cytiva) at 2 ml/min and washed with 3 column volumes (CVs) PBS pH 7.4. Captured protein was eluted with 0.1 M sodium citrate buffer pH 3.6. Eluate was neutralised with 2 M Tris-HCl pH 8.5 and subjected to quality assessments described in the next sections.

Analytical size exclusion ultra-performance chromatography (SE-UPLC)

Solution phase size of proteins was analysed using SE-UPLC by injecting 2 µg purified protein sample onto an ACQUITY BEH200 column (Waters) at a flow rate of 0.35 ml/min and developed with an isocratic gradient of 0.2 M sodium phosphate, pH 7.0. Absorbance at 280 nm and multi-channel fluorescence was used for signal detection. Molecular weight estimation was performed by comparison to gel filtration protein standards (BioRad).

Mass photometry analysis

Measurements were performed using clean glass coverslips (High Precision coverslips, No. 1.5, 24 × 50 mm, Marienfeld) mounted with silicon gaskets (CultureWell™ Reusable Gaskets, Grace biolabs) cut in to 4x2 well sections. Immediately prior to mass photometry measurements, antibody stocks were diluted to approximately 50 nM with Dulbecco's Phosphate-Buffered Saline (DPBS, ThermoFisher). Data were acquired on a Refeyn TwoMP mass photometer (Refeyn Ltd, Oxford, UK) using AcquireMP (Refeyn Ltd, v2.2.1) software and images were processed and analysed using DiscoverMP (v2.3.dev12) software. The instrument lens was cleaned prior to use with Iso-propyl alcohol (IPA), allowed to dry and a drop of Olympus Low Auto Fluorescence Immersion Oil (NC0297589, ThermoFisher) placed on the lens prior to positioning the microscope coverslip with sample in the light stage. To find focus, 15 µl of fresh DPBS was pipetted into a silicone well, the focal position was identified and secured in place with an autofocus system based on total internal reflection for the entire measurement; data were acquired on the buffer prior to each sample dilution to assess background contamination. IgG1 Fc-µtp and IgG1 Fc-µtp L309C were supplied at 44.2 µM. For each acquisition 5 µl of 200 nM dilutions in PBS were introduced into the well, mixed thoroughly, following autofocus stabilization, and movies of 180 s duration recorded. Each sample was measured once and a fresh well and buffer aliquot used to find focus for each measurement.

Sodium dodecyl sulphate polyacrylamide gel electrophoresis (SDS-PAGE)

SDS-PAGE was used to assess the nature of the hexameric profile as observed on SEC i.e. covalent or non-covalent interactions. Approximately 3 µg of protein was prepared by mixing with 4 × NuPAGE LDS sample buffer and either 10 nM N-ethylmaleimide (Thermo Fisher Scientific) or 10 × NuPAGE reducing agent. The prepared sample was denatured at 95 °C for 3 min and loaded on to Novex 4-20% Tris-Glycine Plus WedgeWell gels alongside SeeBlue pre-stained molecular weight marker. Gels were stained with InstantBlue according to the manufacturer's instructions (Expedeon) and imaged using the ImageQuant LAS 4000 system (GE Healthcare).

Peptide mapping for glycan analysis

Samples were reduced using dithiothreitol (Thermo Fisher Scientific) in denaturing conditions with guanidine hydrochloride (Sigma-Aldrich). Free sulfhydryls were capped with iodoacetamide (Thermo Fisher Scientific), before buffer exchange. The buffer exchanged sample was then digested with sequencing grade modified trypsin (Promega) and finally quenched with trifluoroacetic acid (Sigma-Aldrich).

Liquid chromatography electrospray ionisation mass spectrometry was acquired using a Vanquish LC system (Thermo Fisher Scientific) coupled with a Q-Exactive Plus Orbitrap (Thermo Fisher Scientific, Horsham, UK). Separations were performed using gradient elution (A: 0.1% formic acid; B: 0.1% formic acid in acetonitrile) on an Acquity UPLC BEH C18 column (130 Å, 1.7 µm, 2.1 × 150 mm; Waters).

A full MS/dd-MS2 (Top 5) scan was run in positive mode. Full MS: scan range was 200–2000 m/z with 70,000 resolution (at 200 m/z). Data were acquired using Xcalibur™ software (Thermo Fisher Scientific).

Solution phase hexamerisation

Protein formulated in PBS pH 7.4, was concentrated using Amicon® Ultra-15 centrifugal filter units (Sigma-Aldrich). Percentage solution phase hexamer was determined by increasing concentration up to 70 mg/ml for Fc-tp fusions and 20 mg/ml for IgG-tp fusions. Concentrated samples were subjected to analytical SE-UPLC and after peak integration, the area under the curve was calculated as a percentage of the total sample.

HDX-MS

For HDX-MS analysis, 4 µl of either 25 µM of IgG1 Fc, IgG1 Fc-µtp or IgG1 Fc-µtp R355Q were diluted into 57 µL of 10 mM phosphate in H_2O (pH 7.0), or into 10 mM phosphate in D_2O (pD 7.0) at 25 °C. The deuterated samples were then incubated for 0.5, 2, 15 and 60 min at 25°C. After the reaction, all samples were quenched by mixing at 1:1 with a quench buffer (4 M Guanadine Hydrochloride, 250 mM Tris (2-carboxyethyl) phosphine hydrochloride (TCEP), 100 mM phosphate) at 1 °C. The mixed solution was at a final pH of 2.5. The mixture was immediately injected into a nanoAcquity HDX module (Waters Corp). for peptic digest. Peptide digestion was then performed on-line using an enzymatic online digestion column (Waters) in 0.2% formic acid in water at 20 °C with a flow rate of 100 µL/min. All deuterated time points and un-deuterated controls were carried out in triplicate with blanks run between each data-point. Peptide fragments were then trapped using an Acquity BEH C18 1.7 µM VANGUARD chilled pre-column for 3 min. Peptides were then eluted into a chilled Acquity UPLC BEH C18 1.7 µM 1.0 × 100 using the following gradient: 0 min, 5% B; 6 min, 35% B; 7 min, 40% B; 8 min, 95% B, 11 min, 5% B; 12 min, 95% B;

13 min, 5% B; 14 min, 95% B; 15 min, 5% B (A: 0.2% HCOOH in H2O, B: 0.2% HCOOH in acetonitrile. Peptide fragments were ionized by positive electrospray into a Synapt G2-Si mass spectrometer (Waters). Data acquisition was performed in ToF-only mode over an m/z range of 50-2000 Th, using an MSe method (low collision energy, 4V; high collision energy: ramp from 18V to 40V). Glu-1-Fibrinopeptide B peptide was used for internal lock mass correction.

MS^E data from un-deuterated controls samples were used for sequence identification using the Waters Protein Lynx Global Server 2.5.1 (PLGS). Peptide search was performed against a database of the Adalimumab sequence only. Peptides were subjected to further filtering in DynamX. Filtering parameters used were a minimum and maximum peptide sequence length of 4 and 25, respectively, minimum intensity of 1000, minimum MS/MS products of 2, minimum products per amino acid of 0.2, and a maximum MH +error threshold of 10 ppm. DynamX v3.0 was used to quantify the isotopic envelopes resulting from deuterium uptake for each peptide at each time-point. Furthermore, all the spectra were examined and checked visually to ensure correct assignment of m/z peaks and only peptides with a high signal to noise ratios were used for HDX-MS analysis.

Results

Contribution of intermolecular disulphide bonds and N-linked glycans to hexamerisation of IgG1 Fc-µtp fusions

First, we wanted to characterise our fusion molecules for size and investigate the importance of inter-hinge DSBs, inter-µtp DSBs and the combination thereof to in-solution hexamerisation. We designed IgG1 Fc-µtp fusion constructs comprising a core hinge (with 2 inter-hinge DSBs), an IgG1 Fc-µtp with and without L309C (Figure 1B) and expressed them in CHO-SXE cells. The presence of L309C increased the efficiency of hexamer formation by approximately 10%, from 65% to 75% (Figure 2A and 2B). The split peak observed at the typical monomer elution time (~4 min) in analytical SE-UPLC can be attributed to differential glycan occupancy[8] (Table S1). Mass photometry analysis confirmed hexamer molecular weight as 388 kDa and 383 kDa for IgG1 Fc-µtp L309C and IgG1 Fc-µtp, respectively as the main peak with some heterogeneity observed for both molecules (Figure 2C and D). To explore the contribution of inter-hinge, inter-Fc and inter-tp DSBs to these molecules, we mutated cysteine residues in the hinge (C239 and C242), tp (C575) and a combination thereof to serine residues. In agreement with our previous data [8], we showed by SE-UPLC and SDS-PAGE analysis that the critical feature for Fc-hexamer formation was the penultimate µtp Cys residue, C575 (Figure 2B, Figure S2). Mutating both hinge Cys residues to Ser residues did not

appreciably alter the formation of the CHO-SXE secreted hexamer compared to molecules with no hinge modifications: 75% vs 79% and 65% vs 59% for IgG1 Fc-µtp L309C and IgG1 Fc-µtp, respectively. Mutating the tp Cys (C575S) reduced the amount of CHO-SXE secreted hexamer to 21% for IgG1 Fc-µtp L309C. Critically, no hexamer was produced in the absence of the L309C mutation (IgG1 Fc-µtp, Figure 2B and Figure S2D, lane 3). Representative SE-UPLC traces of each molecule are depicted in Figure S2A-C. Taking these and previous data [31] together, they demonstrate that covalent Fc-hexamer formation strictly requires the presence of either C575 or L309C, but both together result in more homogeneous and stable hexamer formation as observed by SDS-PAGE. The hinge DSBs appear to be largely unnecessary for the formation of the covalent Fc-hexamer but influence the overall structure of the hexamer that is formed. No difference in expression levels was observed for the eight different constructs (Figure S3).

The contribution of N-linked glycans in the Fc and tailpiece was also explored. Variants of IgG1 Fc-µtp constructs with and without L309C containing either N297Q in the Fc, N563A in the tailpiece or both were expressed from CHO-SXE cells and purified. SE-UPLC analytics (Figure S4 A and C) confirmed the need for both sites to be glycosylated for stable hexamer formation with the tp glycan being more important. Lanes 3–4 in Figure S4 B and D confirmed the importance of the presence of the tp glycan.

Influence of tailpiece sequence on IgG Fc-tp hexamerisation

We next focussed on the tp sequence using the smaller IgG1 Fc-µtp fusion molecule as a more practicable protein to further understand if particular residues within the tp sequence contributed to hexamerisation efficiency. Human (h) IgG1 Fc was fused to tp sequences from other isotypes and/or species e.g., human IgA1 tp (α1tp), human IgA2 tp (α2tp) and murine µtp (Tables 2 and 3). IgG Fc-µtp fusion proteins were expressed from CHO-SXE cells, and Protein A affinity-purified material analysed by SE-UPLC. hIgG1 Fc fused to either human α1tp or α2tp did not hexamerise well: the major species for both fusions were higher order molecular weight species, most likely soluble 'aggregates' (Figure 3A, middle and bottom panels). Sequence analysis of human µtp and αtp identified seven amino acids that differ between the two tailpieces. Site-directed mutagenesis was performed to introduce individual αtp residues at positions 561, 562, 566, 569, 570, 571, and 572 into hIgG1 Fc-µtp constructs and *vice versa*. Introduction of the αtp-derived residues into the hIgG1 Fc-µtp generally reduced hexamerisation efficiency (summarised in Figure 3B, representative analytical SE-UPLC traces in Figure S5). Closer analysis revealed that hydrophobic residues L561, L562 and L566 may play a central role in stabilising hexamer formation as these µtp to αtp substitutions reduced hexamer percentages expressed from CHO-SXE cells (Figure 3B). L561H resulted in predominantly monomer species, whereas L566V and Y562I/V led to higher order molecular weight

species (dodecamer). S569A resulted in 79% hexamer from CHO-SXE, which was above that seen with the wildtype molecule (66%). Mutations at position 571 (T571A, T571V) yielded similar levels of hexamer to wildtype from CHO-SXE cells (Figure 3B) at 74% and 67% for T571A and T571V, respectively. Substituting (D570E) or introducing (A572D) charged residues both reduced hexamer formation. For A572D, as hexamer formation decreased, monomer formation increased but for D570E, reduced hexamer formation corresponded with an increase in both high molecular weight and monomer species. We also made and tested all of the inverse mutations in the αtp, i.e., introducing μtp residues singly into α1tp and α2tp (Figure S6). As noted above, both α1tp and α2tp fusions result in near complete dodecamer formation. Only V562Y substantially rescued hexamerisation potential of the hIgG Fc-αtp fusion molecule by producing very little dodecamer (12%) and substantial levels (70%) of hexamer (Figure S6). The other substitutions still resulted in substantial amounts of higher order molecular weight species. Together, these data support that residues L561, Y562 and L566 are particularly important for efficient tp-driven IgG hexamer formation. Finally, we mutated every μtp residue to an Ala residue to determine the impact of individual residues on IgG Fc-μtp hexamerisation (Figure 3C). In this experiment, S569A showed the highest level of hexamerisation at 73%; however, this was slightly lower than the 79% observed previously, most likely reflecting differences in transfection efficiency (Figure 3B).

G573A, T571A and T574A, all demonstrated similar or non-significantly higher levels of hexamer formation compared to wildtype suggesting that they are not critically involved in hexamerisation. All other modifications had detrimental effects on hexamerisation either by promoting the formation of higher order molecular weight species (P559A, N563A, S565A and D570A) or by disrupting hexamer formation and predominantly generating monomer (L566A, C575A, V567A, L561A, V564A, Y562A, T560A, and M568A, ranked by higher to lower levels of monomer). The effects of N563A, S565A and C575A were perhaps unsurprising due to their predictable impact of ablation of N-glycosylation and DSB formation, respectively, as both tp glycan and C575 are critical to hexamerisation [11,13]. The strong impact of L561, Y562, and L566, but also V567 on hexamer formation were consistent with the αtp mutagenesis results and previously published data [18].

We next compared human and murine μtp sequences and observed two residue differences at positions 567 (V/I) and 572 (A/G) (Table 3). A panel of variants was generated to investigate these differences by analytical SE-UPLC and ranked according to the percentage hexamer formation (Table 4). Overall, higher levels of hexamer were observed when valine was present at position 567, regardless of the species of the tailpiece or Fc. Human IgG1 Fc fused to murine μtp and murine IgG1 Fc fused to murine μtp molecules

both yielded 52% hexameric species in solution, both lower than the 68% seen for hIgG1 Fc with human µtp (Figures 4A-C, Table 4). This result was somewhat unexpected as there are only two amino-acid differences between human µtp and murine µtp. To investigate this, we mutated these residues within human µtp to murine residues and murine µtp residues to human residues (Table 4). In the context of the hIgG1 Fc-human µtp, only residue V567I disrupted hexamer formation (reduced from 68% to 52%), suggesting that position 567 but not A572 (mutated to G, 65% hexamer) contributes to stabilizing or facilitating hexamer formation. Similarly, in the context of hIgG1 Fc-murine µtp, introducing I567V improved hexamer formation from 47% to 65%. These, and the Ala scanning data, suggest that position 567 is important to tp-driven hexamerisation irrespective of the Fc species whilst position 572 makes a limited contribution.

Together, these data identify that 13 of 18 µtp residues of human µtp are important for hexamerisation potential: P559, T560, L561, Y562, N563, V564, S565, L566, V567, M568, D570, C575 and Y576. In addition, appropriate substitution of S569, T571 and T574 can further enhance hexamerisation efficiency. The IgM Fc structure indicated the importance of the hydrophobic residues in efficient packing which we have now confirmed experimentally (L561, Y562, V564, L566, V567, M568 and Y576) [19]. Furthermore, fusing the murine µtp to either a human or murine IgG1 Fc has a detrimental effect on hexamerisation of these fusion molecules (Figures 4B and C).

Comparison of hexamerisation efficiency of IgG1 and IgG4 Fc µtp fusions and hybrids

Due to our previous observation of differential hexamerisation efficiency between IgG1 and IgG4 [7], we next investigated human isotype differences in detail with SE-UPLC. IgG1 Fc-µtp typically yielded 63% hexamer after CHO cell expression whereas IgG4 Fc-µtp yielded 32% (Figure 5A). Hence, we generated isotype constant region hybrids, swapping domains between isotypes, in order to better determine which domain imparted hexamerisation efficiency. IgG1$_{C\gamma 2}$-IgG4$_{C\gamma 3}$ Fc-µtp and IgG4$_{C\gamma 2}$-IgG1$_{C\gamma 3}$ Fc-µtp molecules were expressed, purified and analysed by SE-UPLC (Figures 5B and C). Substituting the IgG1$_{C\gamma 3}$ with the IgG4$_{C\gamma 3}$, compromised hexamer formation and yielded predominantly monomer species (87% monomer, Figures 5B and S7). Conversely exchanging the IgG4$_{C\gamma 3}$ for the IgG1$_{C\gamma 3}$ domain, recovered hexamer formation to levels similar or greater than IgG1 Fc-µtp (63% hexamer, Figures 5C and S7 vs 32%). These data suggest Cγ3 is a critical determining factor in the efficiency of hexamerisation from CHO-SXE cells.

Identification of R355 in the Cγ3 domain as a key residue for hexamerisation

A Cγ3 protein sequence alignment identified six differences between IgG1 and IgG4 (Figure 5D). Hence, we mutated each different Cγ3 residue to its isotype counterpart and identified R355 as key a residue for efficient hexamerisation (Figure 5E and F). Hexamerisation decreased from 63% in hIgG1 Fc-µtp to 23% for hIgG1 Fc-µtp R355Q (Figures 5E left and S7) whereas hexamerisation improved from 32% in hIgG4 Fc-µtp to 67% for hIgG4 Fc-µtp Q355R (Figures 5F right and S7). The five other mutations had limited impact on hexamerisation efficiency (Figures S8 and S9). Knowing that position 355 was key, we mutated R355 to every other natural amino acid in an IgG1 Fc-µtp construct (an overview is depicted in Figure S10). Introducing a similar positively charged residue, Lys, had minimal impact on hexamerisation efficiency with some increase in dodecamer formation (Figure 5G) whereas introducing negatively charged residues, Asp (Figure 5H, dashed line) or Glu (Figure5HD, dotted line) resulted in notable disruption of hexamer formation, to 7% and 8%, respectively (Figure S10). Introducing a polar, non-charged residue, Ser (R355S), decreased hexamer formation to 27% (Figure 5I, dotted line). Introducing a cysteine (R355C) increased hexamer formation to 85% but the presence of an asymmetrical peak suggested a mixed, undefined hexameric species or soluble aggregates (Figure 5I, dashed line). Additional mutations to every other natural amino acid at position 355 showed no beneficial effect on hexamerisation (Figures S10).

These data demonstrate R355 as a key residue that promotes hexamerisation more so than unmutated hIgG4-µtp fusion molecules. Evidence of DSB formation with R355C implies close spatial proximity between neighbouring R355 residues. To better understand why this residue plays a critical role in hexamer formation, we examined a previously published IgG1 Fc structure (PDB: 1HZH) and noted that this residue is positioned at the base of the Fc (Figures 6A and B). To explore which interactions contribute to enhanced hexamerisation efficiency in IgG1, we compared hIgG1 Fc-µtp and hIgG1 Fc-µtp R355Q using HDX-MS. The HDX-MS analysis revealed that the presence of the tailpiece protects peptides located at the Fc monomer–monomer interface. This suggests that the tail piece drives the individual monomers to multimerise and form contacts with each other. However, upon the R355Q mutation, the same peptide in the interface becomes exposed and experiences increased deuterium uptake. This indicates that the monomers are no longer in contact (Figures 6C and D).

In-solution hexamerisation: comparison of full-length IgG1-µtp, IgG4-µtp and variants

Previous work demonstrated that IgG-tp$_{C575S}$ self-interacts non-covalently in a concentration dependent manner to form hexameric IgG-µtp in-solution [8]. In the previous section we identified R355 as central to hexamerisation efficiency of IgG Fc-µtp fusions. Therefore, here we made combinations of IgG1-µtp$_{C575S}$

with and without R355Q and IgG4-µtp$_{C575S}$ with and without Q355R. Molecules were generated as Fc-µtp and full-length IgG-µtp fusions. For Fc-µtp fusions, material was concentrated up to 70 mg/ml and diluted back to 1 mg/ml to evaluate reversible, non-covalent hexamerisation. Antibodies containing R355 demonstrated hexamer formation of ~50% at 70 mg/ml (Table 5). Conversely, of the material containing Q355 only, ~30% of material was hexamerised in solution. For full-length IgG-µtp constructs containing R355, up to 18% of the material was hexamerised in solution at 20 mg/ml. Conversely, full-length -µtp material with Q355, did not hexamerise at all (Table 5 and Figure S12). These observations are consistent with the hypothesis that R355 enables the non-covalent hexamerisation potential of Fc-µtp and IgG-µtp both upon target binding and in solution. In the presence of C575 these non-covalent interactions become covalently stabilised. Of note, hexamerisation efficiency was lower for full-length IgG antibodies compared to Fc-µtp molecules, possibly due to steric hindrance from the Fab arms.

***In vitro* activity of Rituximab IgG1$_{R355Q}$-µtp$_{C575S}$ and Rituximab IgG4$_{Q355R}$-µtp$_{C575S}$ constructs**

Having established the importance of residue 355 to the hexamerisation potential of full-length IgG, we next wanted to assess if such modulation of in-solution hexamerisation affected 'on-target hexamerisation' and subsequent effector function. We previously demonstrated that Rituximab (RTX) IgG1-µtpp$_{C575S}$ is able to hexamerise in solution and as a result has enhanced C1q recruitment and CDC activity compared to hIgG1 wildtype on target cells, in the absence of increased C1q binding affinity [8]. In order to assess this, we produced IgG1-µtp$_{C575S}$ and IgG4-µtp$_{C575S}$ variants of RTX. To determine if these mutations modulated the inherent C1q binding activity we first performed an ELISA with plate-coated hIgG constructs. Here, neither the IgG1$_{R355Q}$-µtp$_{C575S}$ nor hIgG4$_{Q355R}$-µtp$_{C575S}$ displayed altered levels of C1q binding (Figures 7A and D), indicating that mutating residue 355 does not impact affinity for C1q.

Next, we investigated the ability of these RTX IgG-µtp$_{C575S}$ variants to recruit C1q and initiate CDC activity. To determine C1q binding differences, after target cell binding, a cell-based C1q recruitment assay was performed. Ramos cells were opsonised with the IgG variants and incubated with purified human C1q, which was then detected using flow cytometry with anti-C1q-FITC. Subsequently, these mAb variants were evaluated for their complement-dependent cell killing of opsonised Ramos cells. The hIgG1$_{R355Q}$- µtp$_{C575S}$ demonstrated no significant increase in C1q recruitment (Figure 7B), and a decrease in target cell lysis (Figure 7C). Human IgG4$_{Q355R}$-µtp$_{C575S}$ displayed a greatly increased level of C1q recruitment (Figure 7E) and accordingly resulted in a large increase in CDC over the otherwise inert hIgG4-µtp$_{C575S}$ (Figure 7F).

Mutagenesis of the N-linked glycan site of the µtp and impact on non-covalent hexamerisation efficiency and CDC activity.

We have confirmed the requirement of the N-linked glycan site to stabilise hexamer formation when expressed from the cell (Figure S4). Next, we explored if we altered the glycan profile, this would impact hexamer formation and hence introduced several variants at position 564 to IgG1 Fc-µtp: V564D, V564E, V564F, V564I, V564L V564S, and V564W. In addition, we also modified the serine at position 565 in the NVS motif found in WT µtp to threonine.

SDS-PAGE and SE-UPLC analyses revealed that variations in the N-linked glycan motif significantly influenced the production profile of the antibody variants (Figures 12A and B and Figure S11). Negatively charged residues such as aspartic acid (D) and glutamic acid (E) completely abolished hexamer formation, as did smaller residues like serine (S) and alanine (A). In contrast, hydrophobic residues—phenylalanine (F), leucine (L), and tryptophan (W)—led to increased aggregate formation, while the S565T variant yielded the highest proportion of hexameric species. The glycan profiles of selected variants were analysed (Figure 11C). As expected, IgG1 Fc-µtp without modification showed approximately 60% glycan occupancy, with a substantial proportion of high-mannose species. Similarly, the V564D variant exhibited 67% occupancy; however, its profile was more homogeneous, with a greater degree of processing to complex fucosylated glycans. In contrast, the V564L variant was predominantly unglycosylated. Finally, the S565T variant displayed approximately 75% occupancy but with less processed glycans compared to the wild-type molecule. Notably, the increased hexamer formation observed for S565T suggests that this modification may be the most promising, despite its higher levels of high mannose glycans.

Next, we wanted to confirm that the hexamerisation efficiency translated to full-length IgG-µtp fusions containing C575S. IgG1-µtp$_{C575S}$ variants were made to contain either: V564D, V564L or S565T. First, these variants were assessed for in-solution hexamerisation by concentrating up to 20 mg/ml and performing SE-UPLC analysis. The variant containing V564D did not hexamerise at 20 mg/ml, similar to IgG1 Fc-µtp fusions. The hexamer levels for IgG1-µtp$_{C575S}$, IgG1-µtp$_{C575S}$ V564L and IgG1-µtp$_{C575S}$ S565T showed hexamer levels of 17%, 36% and 49%, respectively (Figures 8A). The N-linked glycan analysis of the tp revealed that the percentage occupied sites decreased from 54% to 36% and 50% for V564D and V564L, respectively, whereas the S565T variant showed almost full occupancy at 96% (Figure 8B). The lack of hexamerisation of the V564D was associated with a lack of CDC activity (Figure 8C). Despite the increased percentage of hexamer in solution, the V564L variant did not show enhanced CDC over WT whereas the S565T showed a maximum of 80% cell lysis compared to 60% for WT (Figure 8C). In summary, S565T improved both hexamerisation efficiency and CDC activity, whereas V564D reduced hexamerisation and V564L increased hexamerisation without enhancing CDC.

Discussion

IgM multimerisation is a complex process that requires covalent and non-covalent interactions and an appropriate glycosylation profile[11,13,15]. The µtp, an 18-amino-acid peptide, fused to the C-terminus of Cµ4, is essential and contains key residues to facilitate the process. The ability of µtp to enable hexamer formation has previously been exploited by addition to IgG or IgG Fc C-termini[24,27,28,32]. Consistent with the reports describing IgM biogenesis, IgG- and Fc-µtp fusions equally rely on L309C, C575 and N-linked glycosylation at N563 to form covalent, correctly folded hexamers. Here, we explored the critical amino-acid residues within the µtp and in combination with the IgG Cγ3 domain explored which features are involved in efficient IgG hexamer. Features tested included DSBs in the IgG1 hinge, Fc and tp, N-linked glycans and key amino acids within and outside Cγ2 and µtp domains. We confirm the critical requirement of tp N563 glycan (but not Cγ2 N297), key hydrophobic µtp amino acids 561–567 and identify R355 at the base of Cγ3 as key for IgG hexamerisation. Indeed, the presence of Gln rather than Arg at position 355 is a key feature which contributes to the overall effector function quiescence of the human IgG4 isotype and the hexamerisation dependent CDC activity of human IgG1.

First, we established that the oligomeric assembly of Fc-µtp fusions with and without L309C mutations was due to both covalent and non-covalent interactions. Fc-µtp fusions both with and without L309C were expressed as up to 80% covalent hexamers from CHO-SXE cells. IgG1 Fc-µtp fusion proteins including L309C can generate hexamer in the absence of inter-tp DSBs, inter-hinge DSBs, or both. IgG1 Fc-µtp fusion proteins (i.e. lacking L309C) are also not dependent upon hinge DSBs for hexamer formation. IgG1 Fc_{L309C}-µtp constructs, containing C575S are secreted as hexamers. IgG1 Fc-$µtp_{C575S}$ or IgG1 Fc- $µtp_{C575A}$ constructs result exclusively in monomer and so clearly demonstrate that non-covalent interactions alone are insufficient to enable hexamer secretion[5,18,26]. Together, these data suggest that L309C or C575S alone can independently ensure covalent Fc-µtp hexamer formation. In summary, non-covalent interactions conferred by correctly folded Fc domains (supported by the hinge DSB) and the µtp make important contributions to the Fc hexamerisation process which are locked in place by DSB formation through either L309C, C575S or both. Since equivalent DSB features are present in IgM, such a 'belt and braces' approach to hexamer assembly serves to underline the evolutionary value of IgM being produced as a high-fidelity hexamer/pentamer.

We subsequently probed the importance of various µtp residues to the efficiency of hexamerisation by fusing hIgG1 Fc to human IgA tp sequences, fusing hIgG1 Fc to murine µtp, and by performing an Ala scanning experiment mutating every residue in the human µtp to an Ala. We found 13 tp residues which

hindered hexamer formation when substituted to an Ala (P559, T560, L561, Y562, N563, V564, L566, V567, M568, D570, Y576, C575, Y576). Previous studies using Ala scanning of murine µtp in the context of L309C, revealed five residues (Y562, V564, L566A, I567, M568) which disrupted covalent hexamer formation[18] and four of these (Y562, V564, L566 and M568) were also previously identified to form part of a hydrophobic patch that stabilises hexamerisation through non-covalent interactions[19]. We generated human/murine µtp hybrids and additionally demonstrated that V567I disrupts hexamer formation whilst reverse engineering of mIgG1 Fc-µtp with the human residue I567V rescued hexamer formation. Pasalic et al. also used Ala scanning mutagenesis of IgM to identify D570 as important, but not essential, for the formation of covalent IgM hexamer formation[18]. We show that the D570A mutation in IgG Fc-µtp fusions led to production of higher molecular weight species whereas mutation to a similarly charged acidic residue, Glu (D570E), reduced efficiency of hexamer formation from ~65% to 50%, suggesting that charge is a major but not the sole contributor to hexamer stability. C575 and N563 have been previously established (and confirmed in this study) as important for covalent hexamer formation through DSBs and N-glycosylation [11,18,26,33]. L561 was identified as important for efficient hexamerisation whilst a further 3 residues (P559, T560, Y576) were shown to play a more limited role in hexamer formation in-solution. P559A leads to higher molecular weight species in-solution whereas the other three disrupt hexamer formation and predominantly form monomer in-solution.

We subsequently investigated how the 7-residue differences between µtp and αtp impacts the hexamerisation of IgG1. Sørensen et al. studied full-length IgG3-µtp both with and without the µtp and the L309C mutation[34]. They showed that the IgG3-µtp and IgG3-µtp L309C fusions both secreted poorly and demonstrated <25% and 80% hexamer, respectively (as assessed by SDS-PAGE, not SE-HPLC). They also showed the importance of L561H and Y562V (HV) mutations, which led to formation of high molecular weight species (i.e. larger than hexamer) whereas L566A, S569A, D570E, T571V and A572D (AAEVD) resulted in more hexamer formation[34]. We deconvoluted the contribution of individual αtp residues with the goal of identification of residues which might lead to maximisation of human µtp hexamer formation. We found that 3 residues are important in hexamer formation: 562V (generating dodecamer or hexamer), 561H, and 566A (leading to hexamer) whilst 569A, 570E, 571V and 572D were not (Figures 3 and S5). Overall, data here are consistent with data from others[17-19] and identify a core cluster of hydrophobic residues in the tp which if mutated can somewhat improve or deleteriously impact hexamer formation.

IgM has five N-linked glycosylation sites in the heavy chain, with the N563 site in the µtp region being particularly important for multimerisation and structural stabilization[13,35]. We show using Fc-µtp fusion

molecules, glycan occupancy of approximately 50% consistent with previous reports. In the absence of µtp glycans (N563A/Q), aggregates were produced from the cell. It has been reported that modifications to the N-linked glycan site can alter glycan occupancy and efficiency [29]. The N-linked glycan site of µtp is $N_{563}V_{564}S_{565}$, and we mutated V564 to various residues, including changing the motif to NVT. The S565T variant promoted enhanced hexamerisation efficiency in IgG1 Fc-µtp and IgG1-µtp fusion molecules. Glycan analysis revealed increased occupancy at N563 and changes in glycan composition.

We also investigated the impact of different human isotypes on hexamerisation. Our data indicated that the hexamerisation efficiency of the hIgG1 Fc-µtp fusion was superior to that of hIgG4 Fc-µtp. We demonstrate that R355 in the Cγ3 of hIgG1 is the key residue that enables its efficient hexamerisation. We postulated that this is attributed to local and most likely inter Fc:Fc interactions at the base of Cγ3 and illustrated this by confirming DSB formation with R355C. Assessing the crystal structures of hIgG1 (1HZH) and the recently published IgM structure (6KXS) we observe that R355 (and IgM's R461) is located at the base of the Ig Fc (Figure 6) [19,23]. Alignment of Cγ3 regions with Cµ4 show that the Cµ4 also contains an arginine at its homologous position 461. Conversely, IgA which dimerises, contains a Glu in this location, also suggestive of the functionality of this position.

We further studied the importance of R355 using both Fc and full-length IgG1 and IgG4 with and without either R355Q or S565T. As expected, IgG1 Fc_{R355Q}-µtp had diminished hexamerisation (23%) compared to wildtype hIgG1 (63%) whereas hIgG4 Fc_{Q355R}-µtp showed significant enhancement of hexamerisation efficiency (67%) compared to wildtype hIgG4 (32%). For full-length IgG, we obtained similar results in the context of IgG-µtp C575S fusions, the percentage hexamerisation in-solution for IgG1- µtp C575S and IgG4-µtp C575S were 16.9% and 18.4%, whereas no hexamerisation was observed for IgG4-µtp and IgG1-µtp R355Q. This was further supported by the ability of the Q355R mutation to confer C1q binding and CDC activity to hIgG4-µtp and somewhat reduced CDC of IgG-tp_{C575S} R355Q. Together these data suggest that Q355 is a key feature involved in the minimisation of IgG4 effector functions. The immune quiescence of hIgG4 is known to involve multiple additive features: weak C1q and FcγR binding in Cγ2and monovalent target binding *via* Fab arm exchange; all of which contribute to the effector-reduced character of hIgG4. Here we add low inherent potential to form the hexamers required for CDC, due to Q355. Mutation to Q355R which is distant from the C1q binding site significantly increases the ability of IgG4 to perform CDC. Overall, we show that R355 found in human IgG1, 2 and 3 is permissive for IgG hexamerisation whilst Q355 is non-permissive with important consequences for CDC activity.

The IgM tailpiece has found utility in drug discovery as a fusion partner on human Fc and IgG as a means to promote both covalent (C575) and non-covalent, concentration or on-target dependent (C575S) hexamerisation of both Fc and full-length IgG fusions [20, 23, 33]. These have been considered as possible therapeutic modalities for FcγR and C1q blockade, enhanced antigen specific CDC and clustering induced receptor agonism. Past research efforts had focussed on restricted tailpiece sequence features and were difficult to translate into drug discovery insights, since they had been undertaken in the background of IgM or IgA Hence our goal was to thoroughly explore all aspects of tailpiece biology, using human IgM and IgA tp inter-species comparisons and ultimately human isotype comparisons. We found and confirmed that essential features for high fidelity hexamerisation was a group of core hydrophobic residues and the N563 N-linked glycan. The penultimate cysteine (C575) was dispensable for hexamerisation in general, but essential for covalent hexamer formation. Many tp mutations result in worsened hexamerisation, including poor expression, inefficient hexamerisation and formation of high molecular weight species and aggregates. A small number of mutations increased hexamer formation efficiency, although the improvement was generally modest, typically around 10%.

In the course of this work, we uncovered two unique insights. First, high levels of glycan occupancy of the N563 tp site were shown by a previously undescribed S565T mutation, found within the N-X-S/T motif. This mutation resulted in increased hexamerisation potential for both covalent and non-covalent hexamers and was shown to both increase N563 occupancy but also for covalent hexamers (C575) result in a change in glycan composition to more high mannose forms. We were unable to elucidate whether either, or both were the important factors but propose higher occupancy as the likely driver. Aglycosyl tailpieces result in HWMS and aggregate. High mannose could simply bear witness to a faster / more complete hexamerisation within the CHO cell secretion pathway and hence reflect access to glycan processing enzymes. Secondly, of wider interest to the antibody community was the striking involvement of position 355 of the Cγ3 domain in IgG hexamerisation and specifically that Q355 is the major determinant of IgG4's inability to hexamerise. The involvement of Cγ2 sequence motifs and functional monovalency have long been known to abrogate IgG4's CDC, but here we describe a third and possibly dominant feature. When hexamerisation of IgG4(P) is derestricted with a Q355R mutation and aided by a non-covalent tp fusion, an IgG4(P) version of rituximab became very effective at CDC with its potency being only approximately half a log less than a direct IgG1-tp C575S comparator. Overall, our insights provide additional insights and pathways for the development of research tool molecules and therapeutic

IgG which rely on multimerisation for enhanced functional activity such as avid target blocking, CDC or receptor agonism.

Data availability

All data reported in this data are available from the corresponding author by reasonable request.

Code availability

This study did not generate or use any original code.

Acknowledgements

Thanks to R. Griffin, M. Parkinson, A. Turner, and A. Ventom for their early experiments, which significantly contributed to the development of this work.

The study was funded by UCB.

Conflict of interest

MSC is a retained consultant for BioInvent International and has performed educational and advisory roles for Roche, Boehringer Ingelheim, Baxalta, Merck KGaA and GLG. He has received research funding from Bioinvent, Roche, Gilead, iTeos, UCB and GSK.

Author contributions

SJP JMS, JE, ZA, HH, AH and BH designed and performed experimental work. MSC and DPH contributed in the design of experiments. SJP and DPH wrote the manuscript with contributions from MSC. All authors critically reviewed the manuscript.

References

1 Brennan, F. R. *et al.* Impact of antibody Fc engineering on translational pharmacology, and safety: insights from industry case studies. *MAbs* **17**, 2505092 (2025). https://doi.org/10.1080/19420862.2025.2505092

2 Stone, C. A., Jr., Spiller, B. W. & Smith, S. A. Engineering therapeutic monoclonal antibodies. *J Allergy Clin Immunol* **153**, 539-548 (2024). https://doi.org/10.1016/j.jaci.2023.11.018

3 Abdeldaim, D. T. & Schindowski, K. Fc-Engineered Therapeutic Antibodies: Recent Advances and Future Directions. *Pharmaceutics* **15** (2023). https://doi.org/10.3390/pharmaceutics15102402

4 Foss, S. *et al.* Human IgG Fc-engineering for enhanced plasma half-life, mucosal distribution and killing of cancer cells and bacteria. *Nat Commun* **15**, 2007 (2024). https://doi.org/10.1038/s41467-024-46321-9

5 Blundell, P. A., Lu, D., Dell, A., Haslam, S. & Pleass, R. J. Choice of Host Cell Line Is Essential for the Functional Glycosylation of the Fc Region of Human IgG1 Inhibitors of Influenza B Viruses. *J Immunol* **204**, 1022-1034 (2020). https://doi.org/10.4049/jimmunol.1901145

6 Frischauf, N. *et al.* Complement activation by IgG subclasses is governed by their ability to oligomerize upon antigen binding. *Proc Natl Acad Sci U S A* **121**, e2406192121 (2024). https://doi.org/10.1073/pnas.2406192121

7 Qureshi, O. S. *et al.* Multivalent Fcgamma-receptor engagement by a hexameric Fc-fusion protein triggers Fcgamma-receptor internalisation and modulation of Fcgamma-receptor functions. *Sci Rep* **7**, 17049 (2017). https://doi.org/10.1038/s41598-017-17255-8

8 Sopp, J. M. *et al.* On-target IgG hexamerisation driven by a C-terminal IgM tail-piece fusion variant confers augmented complement activation. *Commun Biol* **4**, 1031 (2021). https://doi.org/10.1038/s42003-021-02513-3

9 Ugurlar, D. *et al.* Structures of C1-IgG1 provide insights into how danger pattern recognition activates complement. *Science* **359**, 794-797 (2018). https://doi.org/10.1126/science.aao4988

10 Randall, T. D., Brewer, J. W. & Corley, R. B. Direct evidence that J chain regulates the polymeric structure of IgM in antibody-secreting B cells. *J Biol Chem* **267**, 18002-18007 (1992).

11 Sitia, R. *et al.* Developmental regulation of IgM secretion: the role of the carboxy-terminal cysteine. *Cell* **60**, 781-790 (1990). https://doi.org/10.1016/0092-8674(90)90092-s

12 Mestecky, J. & Schrohenloher, R. E. Site of attachment of J chain to human immunoglobulin M. *Nature* **249**, 650-652 (1974). https://doi.org/10.1038/249650a0

13 de Lalla, C., Fagioli, C., Cessi, F. S., Smilovich, D. & Sitia, R. Biogenesis and function of IgM: the role of the conserved mu-chain tailpiece glycans. *Mol Immunol* **35**, 837-845 (1998). https://doi.org/10.1016/s0161-5890(98)00073-x

14 Muraoka, S. & Shulman, M. J. Structural requirements for IgM assembly and cytolytic activity. Effects of mutations in the oligosaccharide acceptor site at Asn402. *J Immunol* **142**, 695-701 (1989).

15 Davis, A. C., Roux, K. H., Pursey, J. & Shulman, M. J. Intermolecular disulfide bonding in IgM: effects of replacing cysteine residues in the mu heavy chain. *EMBO J* **8**, 2519-2526 (1989). https://doi.org/10.1002/j.1460-2075.1989.tb08389.x

16 Muller, R. *et al.* High-resolution structures of the IgM Fc domains reveal principles of its hexamer formation. *Proc Natl Acad Sci U S A* **110**, 10183-10188 (2013). https://doi.org/10.1073/pnas.1300547110

17 Wiersma, E. J. & Shulman, M. J. Assembly of IgM. Role of disulfide bonding and noncovalent interactions. *J Immunol* **154**, 5265-5272 (1995).

18 Pasalic, D. *et al.* A peptide extension dictates IgM assembly. *Proc Natl Acad Sci U S A* **114**, E8575-E8584 (2017). https://doi.org/10.1073/pnas.1701797114

19 Li, Y. *et al.* Structural insights into immunoglobulin M. *Science* **367**, 1014-1017 (2020). https://doi.org/10.1126/science.aaz5425
20 Klimovich, V. B. IgM and its receptors: structural and functional aspects. *Biochemistry (Mosc)* **76**, 534-549 (2011). https://doi.org/10.1134/S0006297911050038
21 Brezski, R. J. & Georgiou, G. Immunoglobulin isotype knowledge and application to Fc engineering. *Curr Opin Immunol* **40**, 62-69 (2016). https://doi.org/10.1016/j.coi.2016.03.002
22 Shulman, M. J., Collins, C., Pennell, N. & Hozumi, N. Complement activation by IgM: evidence for the importance of the third constant domain of the mu heavy chain. *Eur J Immunol* **17**, 549-554 (1987). https://doi.org/10.1002/eji.1830170418
23 Saphire, E. O. *et al.* Crystal structure of a neutralizing human IGG against HIV-1: a template for vaccine design. *Science* **293**, 1155-1159 (2001). https://doi.org/10.1126/science.1061692
24 Smith, R. I. & Morrison, S. L. Recombinant polymeric IgG: an approach to engineering more potent antibodies. *Biotechnology (N Y)* **12**, 683-688 (1994). https://doi.org/10.1038/nbt0794-683
25 Smith, R. I., Coloma, M. J. & Morrison, S. L. Addition of a mu-tailpiece to IgG results in polymeric antibodies with enhanced effector functions including complement-mediated cytolysis by IgG4. *J Immunol* **154**, 2226-2236 (1995).
26 Blundell, P. A., Le, N. P. L., Allen, J., Watanabe, Y. & Pleass, R. J. Engineering the fragment crystallizable (Fc) region of human IgG1 multimers and monomers to fine-tune interactions with sialic acid-dependent receptors. *J Biol Chem* **292**, 12994-13007 (2017). https://doi.org/10.1074/jbc.M117.795047
27 Czajkowsky, D. M. *et al.* Developing the IVIG biomimetic, hexa-Fc, for drug and vaccine applications. *Sci Rep* **5**, 9526 (2015). https://doi.org/10.1038/srep09526
28 Mekhaiel, D. N. *et al.* Polymeric human Fc-fusion proteins with modified effector functions. *Sci Rep* **1**, 124 (2011). https://doi.org/10.1038/srep00124
29 Shakin-Eshleman, S. H., Spitalnik, S. L. & Kasturi, L. The amino acid at the X position of an Asn-X-Ser sequon is an important determinant of N-linked core-glycosylation efficiency. *J Biol Chem* **271**, 6363-6366 (1996). https://doi.org/10.1074/jbc.271.11.6363
30 Cain, K. *et al.* A CHO cell line engineered to express XBP1 and ERO1-Lalpha has increased levels of transient protein expression. *Biotechnol Prog* **29**, 697-706 (2013). https://doi.org/10.1002/btpr.1693
31 Rowley, T. F. *et al.* Engineered hexavalent Fc proteins with enhanced Fc-gamma receptor avidity provide insights into immune-complex interactions. *Commun Biol* **1**, 146 (2018). https://doi.org/10.1038/s42003-018-0149-9
32 Wang, Q. *et al.* Enhancement of antibody functions through Fc multiplications. *MAbs* **9**, 393-403 (2017). https://doi.org/10.1080/19420862.2017.1281505
33 Della Corte, E. & Parkhouse, R. M. Biosynthesis of immunoglobulin A (IgA) and immunoglobulin M (IgM). Requirement for J chain and a disulphide-exchanging enzyme for polymerization. *Biochem J* **136**, 597-606 (1973). https://doi.org/10.1042/bj1360597
34 Sorensen, V. *et al.* Effect of the IgM and IgA secretory tailpieces on polymerization and secretion of IgM and IgG. *J Immunol* **156**, 2858-2865 (1996).
35 Wang, W. *et al.* Human IgG Subclasses Differ in the Structural Elements of Their N-Glycosylation. *ACS Cent Sci* **10**, 2048-2058 (2024). https://doi.org/10.1021/acscentsci.4c01157

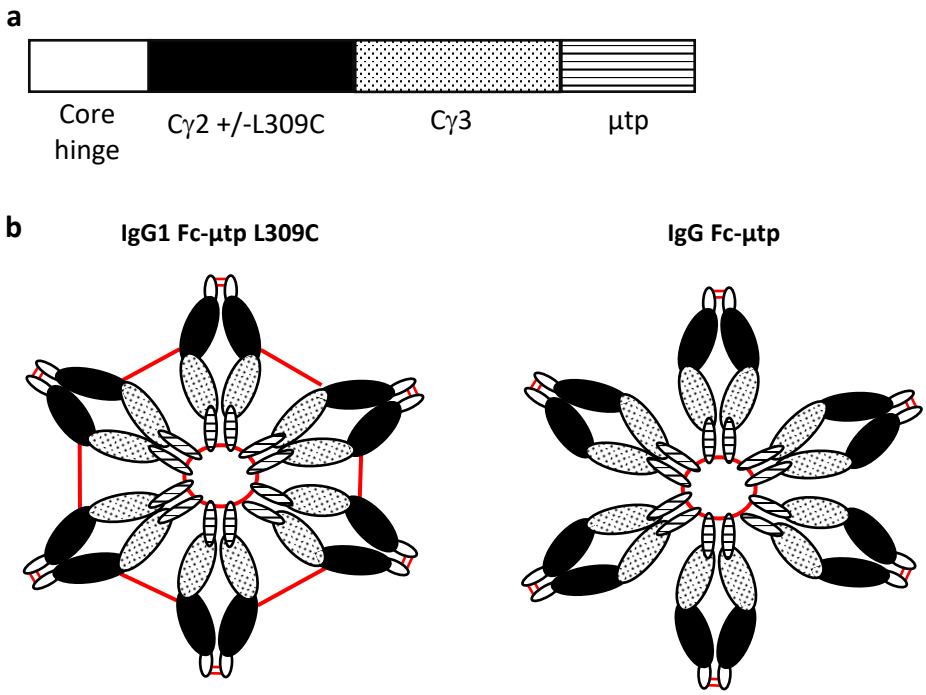


Figure 1. Schematic representation of **(A)** a single subunit of an IgG Fc-IgM tailpiece (μtp) fusion. This comprises an IgG1 core hinge (CPPC), the IgG1 Cγ2 with or without the L309C variant, the IgG1 Cγ3 and the μtp (PTLYNVSLVMSDTAGTC$_{575}$Y). **(B)** Illustration of Fc hexamers represented either in the presence (left) or absence (right) of L309C. Red lines indicate disulphide bonds.

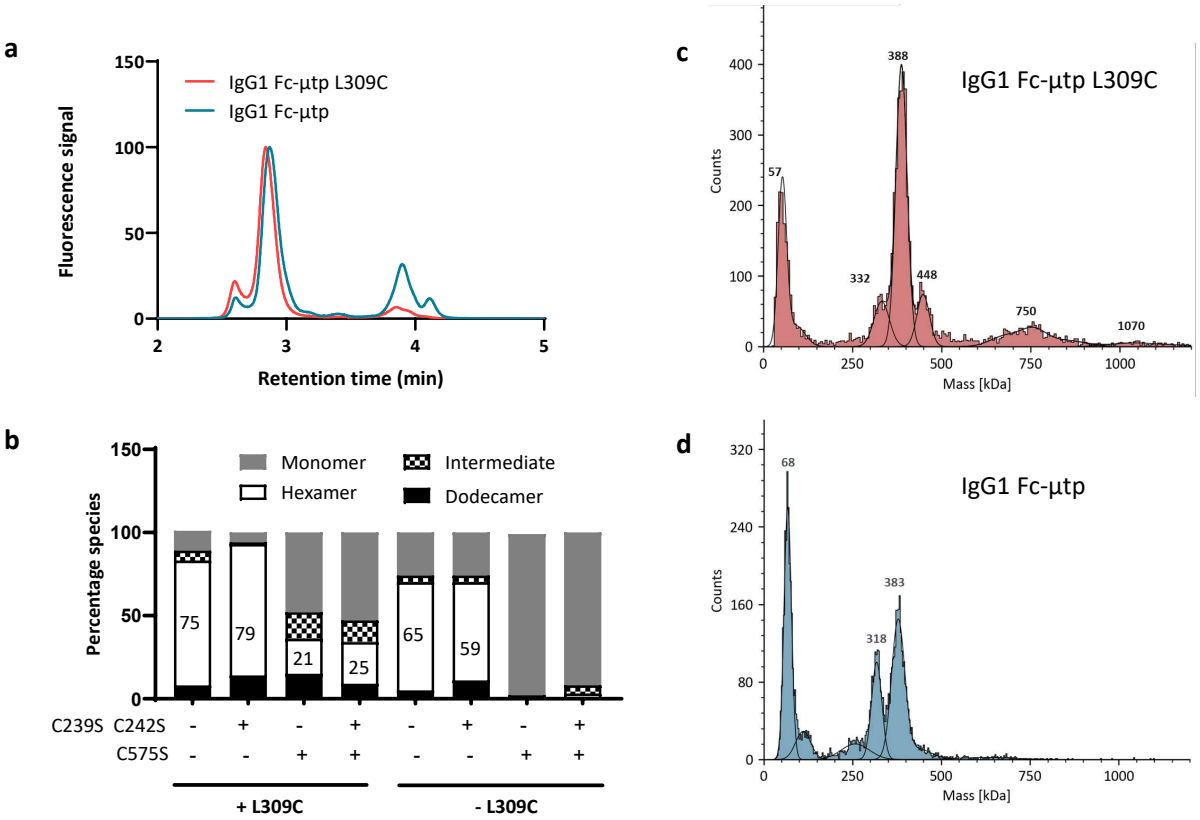


Figure 2. Contribution of inter disulphide bonds to hexamer formation of IgG1 Fc-µtp fusions. IgG1 Fc-µtp fusion constructs comprising a core hinge (with 2 inter-hinge disulphide bonds), an IgG1 Fc and an µtp with or without L309C were expressed from CHO-SXE cells and analysed by analytical SE-UPLC. **(A)** Representative analytical SE-UPLC trace of an IgG1 Fc-µtp with and without L309C. Presence of L309C marginally improves hexamer formation in-solution **(B)** Analytical SE-UPLC data of IgG1 Fc-tp with and without L309C either with hinge mutations (C239S and C242S) and tp (C575S) mutation and both hinge and tp mutations (C239S, C242S and C575S). Numbers represent percentage species after peak integration of SE-UPLC profiles as eluted from the column. Approximate sizing was performed by comparison to protein gel filtration standards and integrated peak species assigned monomer (~50 kda), intermediate (50-300kDa), hexamer (~300 kDa) and dodecamer (>300 kDa). N=3 from independent experiments. **(C+D)** Molecular weights determined by mass photometry (Refeyn) for IgG1 Fc-µtp L309C **(C)** and IgG1 Fc-µtp **(D)**.

Table 2. Comparison of IgM and IgA-tp fusions. Human IgG1 Fc was fused to tp sequences from human (h) IgA1(α1)-tp, or hIgA2(α2)-tp, expressed in CHO-SXE cells, affinity purified and subjected to analytical SE-UPLC. μtp, α1- and α1-tp sequences are listed and aligned. Residues in α1- and α2-tp sequences that differ from μtp are highlighted in red. Percentage hexamer formation as produced in CHO-SXE cells post affinity purification is listed alongside the respective molecules. N=3 from three independent experiments.

Description	Tailpiece sequence	Percentage hexamer from cell (+/- std dev)
hIgG1 Fc-μtp	^{559}PTLYNVSLVMSDTAGTCY^{576}	**65** +/-4.6
hIgG1 Fc-α1tp	^{559}PTHVNVSVVMAEVDGTCY^{576}	**25** +/-5.2
hIgG1 Fc-α2tp	^{559}PTHINVSVVMAEADGTCY^{576}	**20** +/-1.7

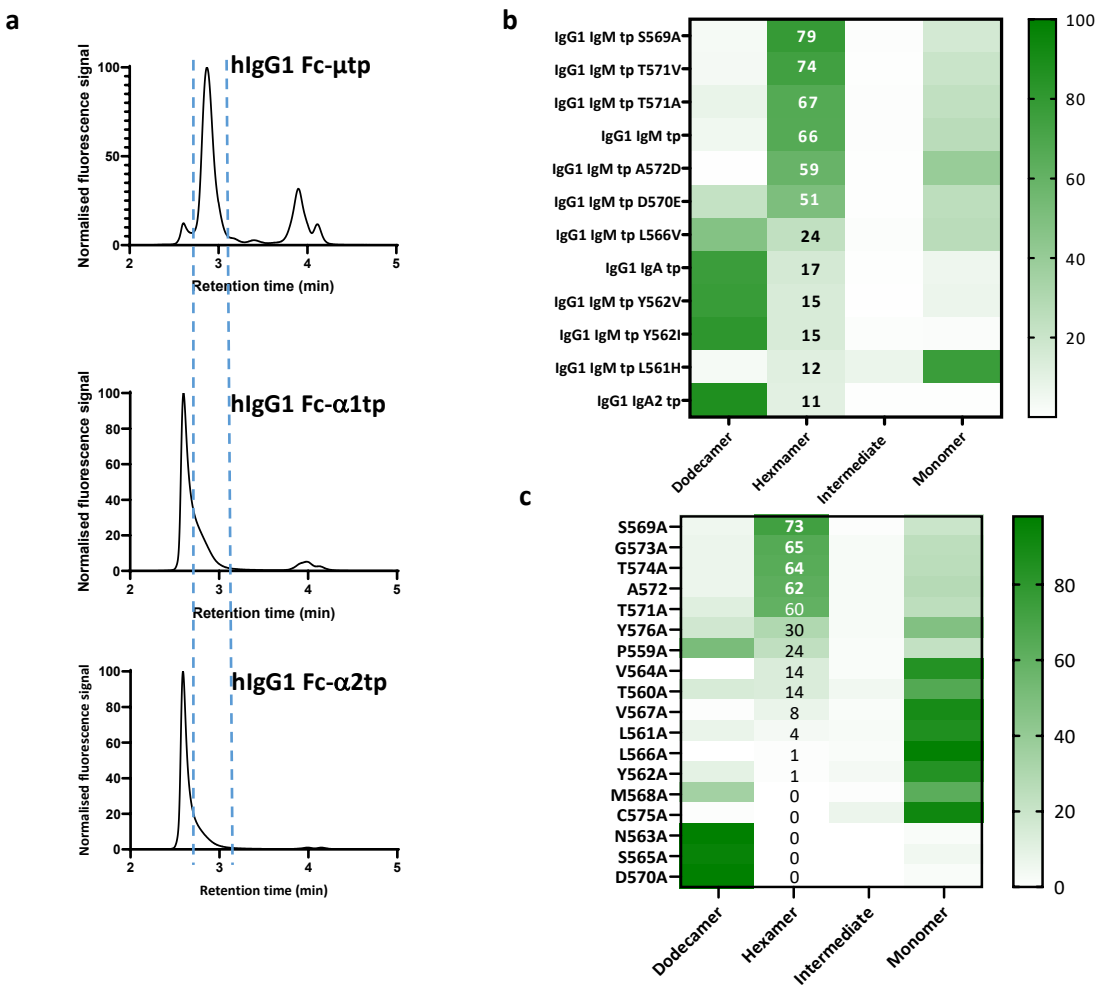


Figure 3. Impact of tp sequences on hexamerisation efficiency. Human IgG1 Fc was fused to tp sequences from human (h) α1tp, or α2tp, expressed in CHO-SXE cells, affinity purified and subjected to analytical SE-UPLC. **(A)** Comparison of representative analytical SE-UPLC traces of hIgG1 Fc fused to a hμtp (top), α1tp (middle) or α2tp (bottom) show αtp fusions to IgG1 Fc do not permit efficient hexamer formation. Hexamer retention time is presented by dashed blue line. **(B)** Heatmap of the percentage dodecamer, hexamer, intermediate and monomer species after integration of analytical SE-UPLC profiles of hIgG1 Fc-μtp mutated towards α1 or α2 tp residues. **(C)** Heatmap of percentage dodecamer, hexamer, intermediate and monomer species after integration of analytical SE-UPLC profiles of hIgG1 Fc-μtp residues mutated alanine. Percentage hexamer was determined by peak integration and calculating area under the curve as a percentage of the whole surface area. Data for figures 3B and 3C generated from two independent experiments.

Table 3. Comparison of µtp sequences from human and mouse. Human and murine tp sequences are listed and aligned below. Two residue differences were identified at positions 567 (V/I) and 572 (A/G) are highlighted in red.

Description	Tailpiece sequence
Human µtp	^{559}PTLYNVSLVMSDTAGTCY^{576}
Murine µtp	^{559}PTLYNVSL**I**MSDT**G**GTCY^{576}

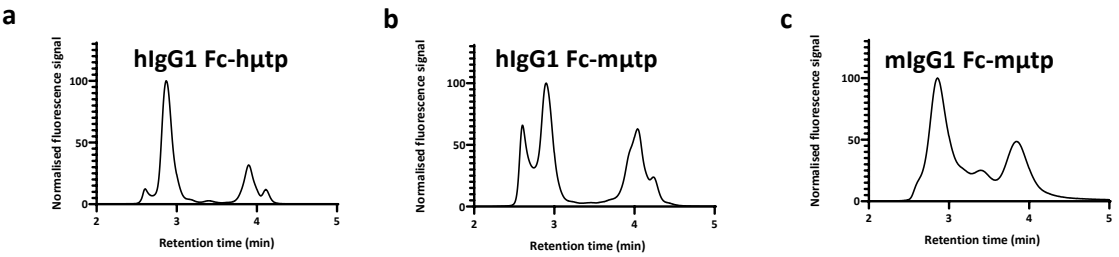


Figure 4. SE-UPLC analysis to determine percentage hexamer post affinity purification of human or murine IgG Fc-µtp hybrid molecules. Human or murine IgG1 Fc was fused to either human (h) µtp or murine (m) µtp, expressed in CHO-SXE cells, affinity purified and subjected to analytical SE-UPLC. Comparison of representative analytical SE-UPLC profiles of hIgG1 Fc fused to **(A)** hµtp **(B)** mµtp and **(C)** mIgG1 Fc-mµtp. Data show the decreased hexamerisation efficiency when fusing a mµtp to either hIgG1 or mIgG1 Fc.

Table 4. Comparison of hexamer formation of variants of hµtp sequence towards residues found in mouse tp. Human IgG1 Fc was fused to tp sequences from human (h) or mouse (m), expressed in CHO-SXE cells, affinity purified and subjected to analytical SE-UPLC. The presence of either a Val or Iso at position 567 and presence of Ala or Gly at position 572 are indicated. Percentage hexamer formation of human IgG1 Fc-µtp fusions produced in CHO-SXE cells post affinity purification is ranked alongside the respective molecules. N=3 from independent experiments.

Fc species	Residue at position		Percentage hexamer formation (+/- Std Dev)
	567	572	
Human	Val	Ala	68 +/- 2.0
Human	Val	Gly	65 +/- 3.0
Murine	Val	Gly	65 +/- 3.1
Murine	Val	Ala	ND
Human	Iso	Ala	52 +/- 3.4
Human	Iso	Gly	52 +/- 1.1
Murine	Iso	Ala	47 +/- 3.5
Murine	Iso	Gly	52 +/-5.1

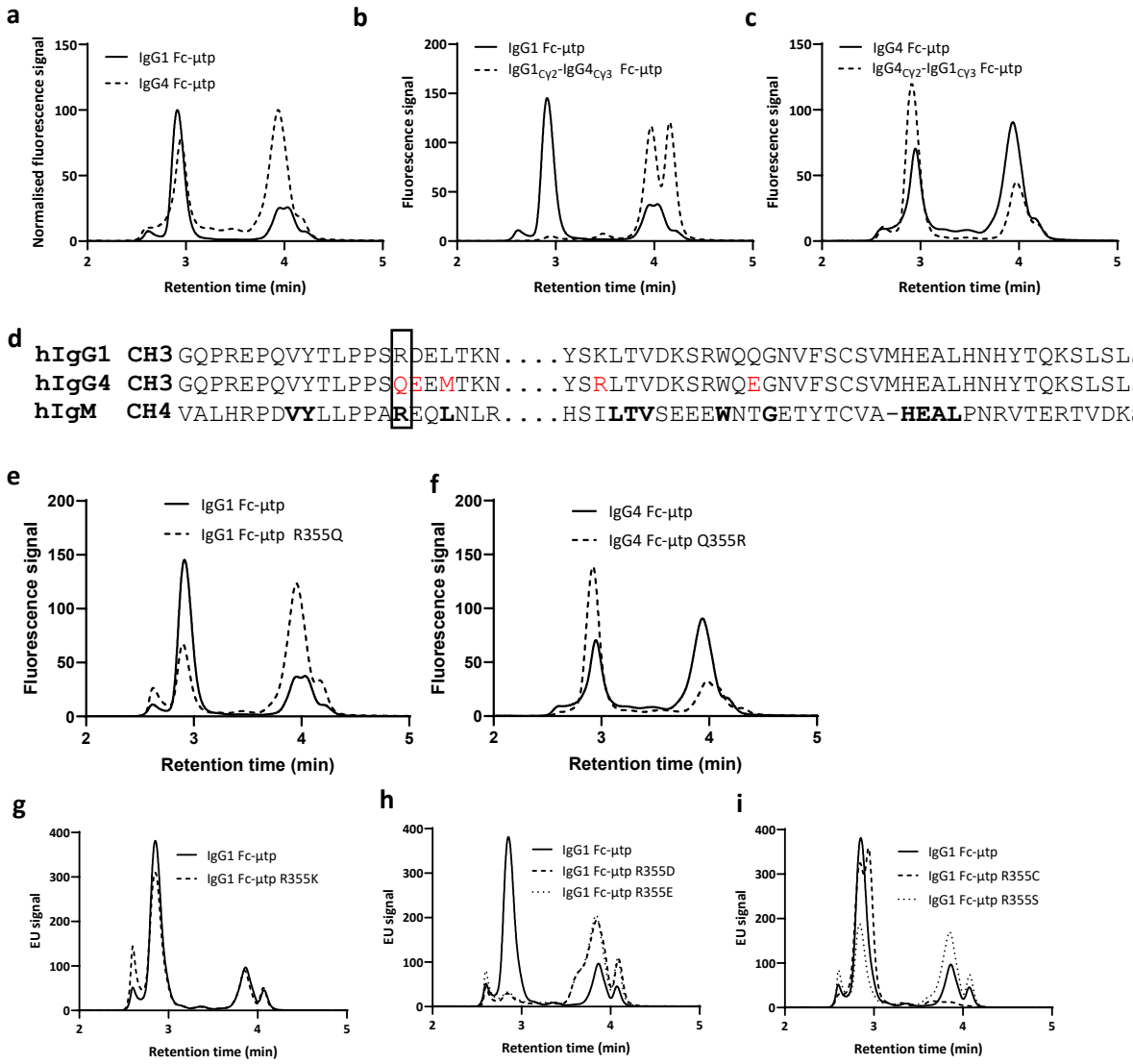


Figure 5. Contribution of the Cγ3 residues within the sequence on hexamerisation efficiency. IgG1 or IgG4 Fc was fused to µtp, expressed in CHO-SXE cells, affinity purified and subjected to analytical SE-UPLC. **(A)** IgG1 Fc-µtp constructs (solid black line) SE-UPLC trace overlaid with IgG4 Fc-µtp (dotted black line). **(B)** SE-UPLC traces of $IgG1_{C\gamma2}$-$IgG4_{C\gamma3}$ Fc-µtp hybrid molecules compared to IgG1 Fc-µtp. **(C)** SE-UPLC traces of $IgG4_{C\gamma2}$-$IgG1_{C\gamma3}$ Fc-µtp hybrid molecules. Experiment was performed in triplicate; each figure shows a representative trace of one experiment. Human IgG1 or IgG4 Fc with various mutations were fused to the µtp, expressed in CHO-SXE cells, affinity purified and subjected to analytical SE-UPLC. **(D)** A protein sequence alignment of hIgG1 and hIgG4 Cγ3 domains and Cµ4 domain. Differences between IgG1 and IgG4 highlighted in red in the IgG4 sequence. Common residues between IgG1 and IgM in bold in the IgM sequence. **(E)** Analytical SE-UPLC of an IgG1 Fc-µtp (solid line) overlaid with IgG1 Fc-µtp R355Q (dotted line). **(F)** Analytical SE-UPLC IgG4 Fc mutated to Q355R fused to µtp (dashed line, right) improves hexamerisation efficiency from the cell as determined by SE-UPLC compared to IgG4 Fc-µtp (solid line, right). Additional mutations within IgG1 Fc illustrating the necessity of a positively charged residue at that position for improved hexamerisation. **(G)** R355K (dashed line) **(H)** R355D (dashed line) and R355E (dotted line) and **(I)** R355C (dashed line) and R355S (dotted line). Each figure depicts a representative trace.

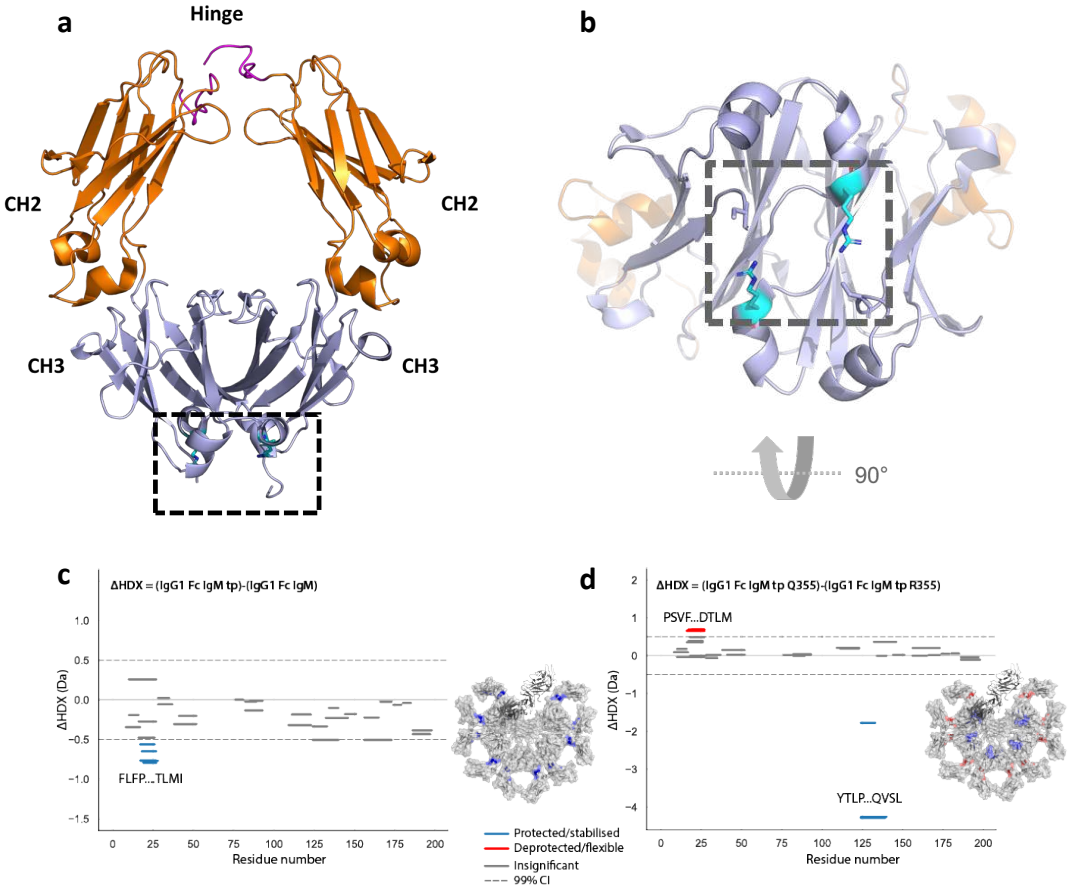


Figure 6. Crystal structure of hIgG1 (PBD IHZH) highlighting the position of R355. (A) Fc crystal structure with hinges depicted in pink, Cγ2 domains in orange and Cγ3 domain in blue. **(B)** Enlargement of the base of the Cγ3 and rotated 90º to further illustrate R355 in cyan. Epitope mapping by HDX-MS**.** Woods plot displaying the differential HDX (ΔHDX) plots for **(C)** IgG1 with and without µtp and **(D)** in the presence of the R355Q mutation. Protected peptides with decreased HDX between states are shown in blue and deprotected peptides with increased HDX between states are shown in red. Peptides with insignificant ΔHDX are represented in grey. ΔHDX has been plotted onto PDB 6KXS for visualisation.

Table 5. Modification of residue 355 alters the hexamerisation potential of Fc and full-length IgG-µtp fusions. Fc or full length IgG1 or IgG4, containing various mutations were fused to the µtp, expressed in CHO-SXE cells, affinity purified and subjected to SE-UPLC analysis. In-solution hexamerisation was measured by concentrating **(A)** hIgG1-µtp C575S, **(B)** hIgG1-µtp C575S/R355Q, **(C)** hIgG4-µtp C575S, and **(D)** hIgG4-µtp C575S Q355R up to 70 mg/ml for IgG1 Fc-µtp fusions and up to 20 mg/ml for full length IgG1-µtp fusions. Percentage of monomeric and multimeric species were calculated by peak integration. Data from N=1

		Mutation	20 mg/ml	70 mg/ml
Fc	IgG1-µtp	C575S	41	52
		C575S R355Q	13	25
	IgG4-µtp	C575S	7	33
		C575S R355Q	40	47
Full length	IgG1-µtp	C575S	17	nd
		C575S R355Q	0	nd
	IgG4-µtp	C575S	0	nd
		C575S R355Q	18	nd

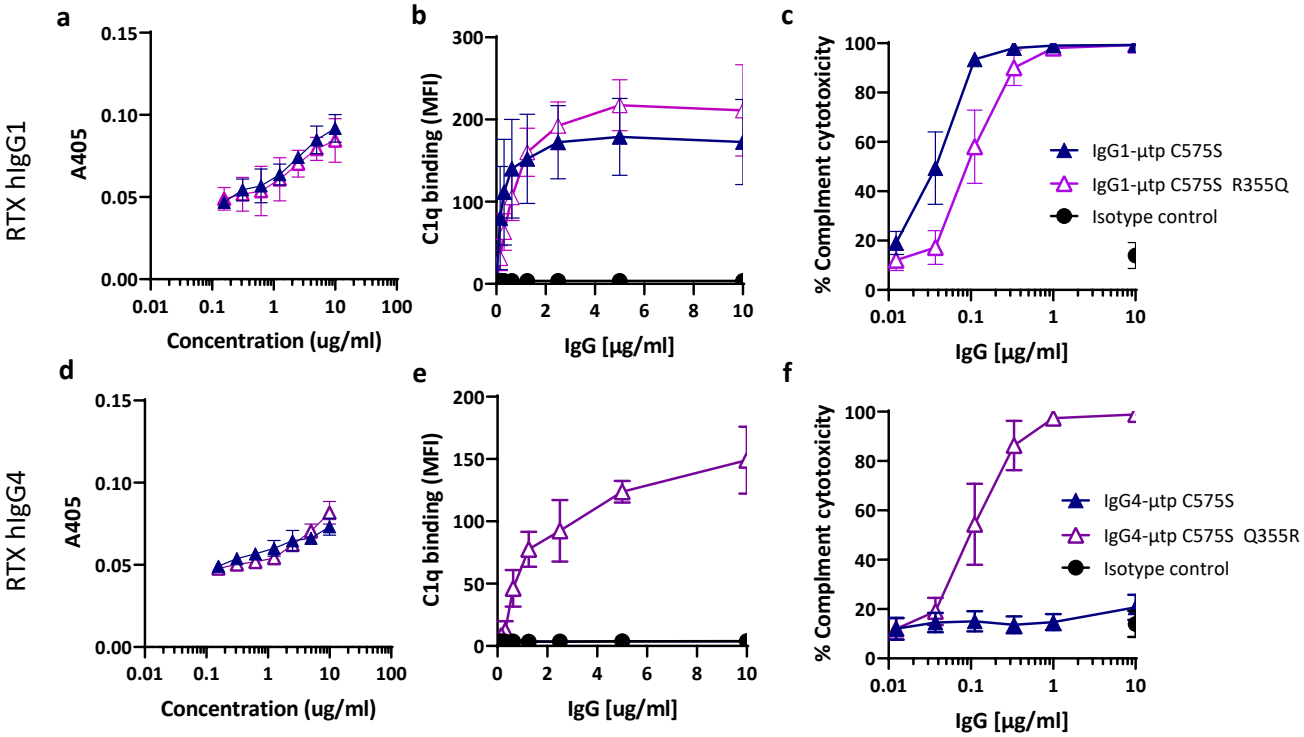


Figure 7. Improved hexamerisation efficiency of hIgG4-µtp C575S can augment CDC activity. C1q binding, C1q cell recruitment, and CDC activity were investigated for RTX IgG1-µtp C575S R355Q (top panel), and RTX IgG4-µtp C575S Q355R(bottom panel). **(A+D)** C1q binding was measured by ELISA (left). ELISA plates were coated with RTX µtp C575S (CS) constructs at various concentrations and purified human C1p (2 µg/ml) was added. Bound C1q was detected with a goat anti-C1q, followed by an anti-goat-HRP conjugated antibody. Data shows absorbance at 405 nm. **(B+E)** C1q cell recruitment was assessed by opsonising Ramos cells with Rituximab (RTX) µtp CS constructs, followed by incubation with 2 µg/ml human C1q. Deposition of C1q was analysed by secondary staining with an anti-C1q-FITC antibody. Data shown is mean and SEM (N=3). CDC-induced cell death (right) was assessed by opsonising Ramos cell with RTX IgG IgM tp constructs and incubated with NHS (20 % V/V). Cell death was examined as the percentage of PI positive cells by flow cytometry. Data shown is mean and SEM (N=4).

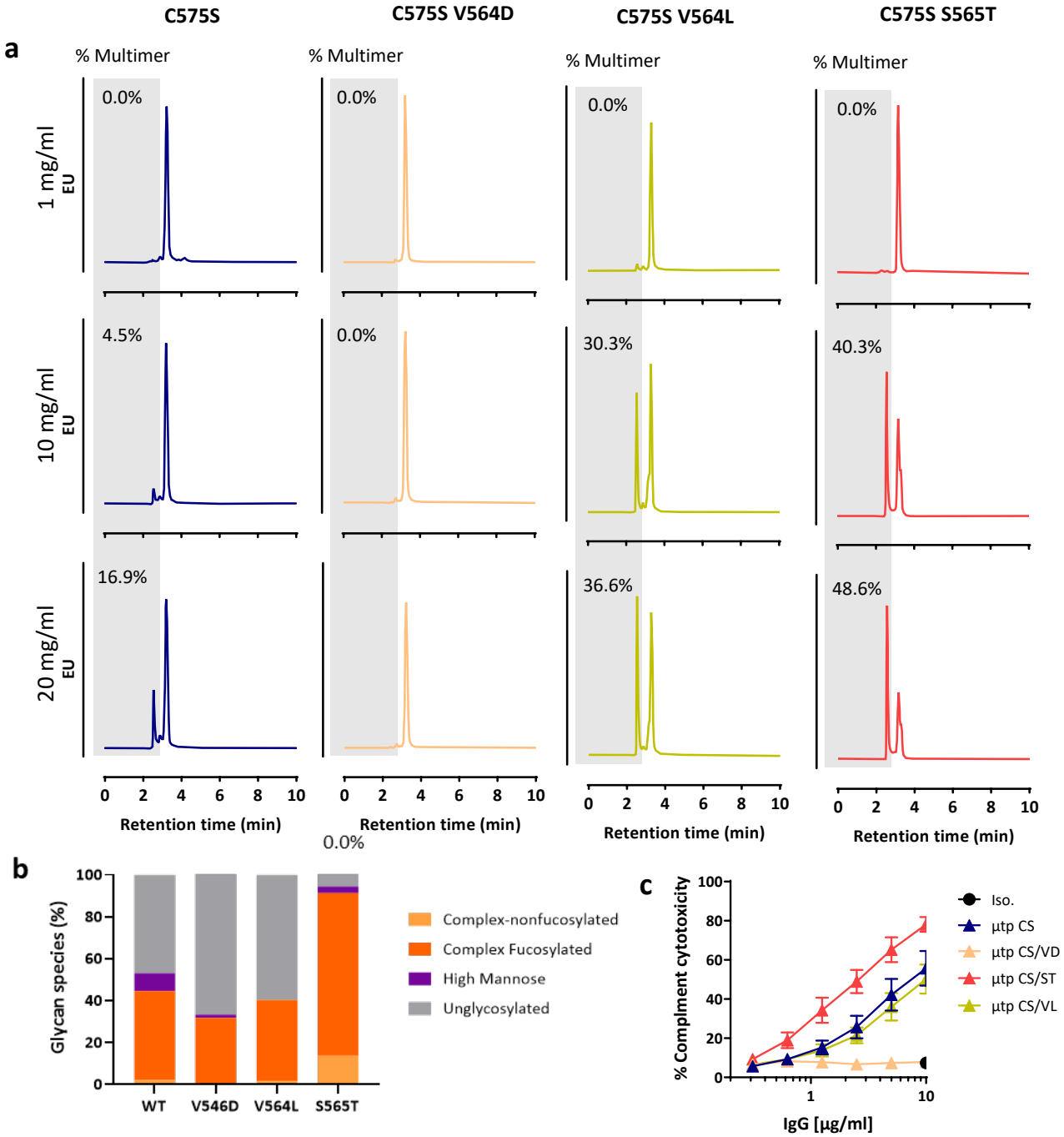


Figure 8. Altering the µtp N-linked glycan occupancy modifies the mAb in-solution hexamerisation efficiency. **(A)** Glycan profiling was undertaken using mass spectrometry of the CH2 and µtp glycan of RTX hIgG1 µtp CS, µtp CS/VD, µtpCS/ST, and µtp CS/VL **(B)** In-solution hexamerisation was measured by concentrating IgG1-µtp CS, IgG1-µtp CS/VD, IgG1-µtp CS/ST and IgG1-µtp CS/VL mAb up to 20 mg/ml and diluted to be analysed by SE-UPLC, and the percentage of monomeric and multimeric species calculated by peak integration. **(C)** Raji cells were opsonised with RTX hIgG1-µtp CS constructs and incubated with NHS (20% V/V). Cell death was examined as the percentage of PI positive cells by flow cytometry. Data shown is mean and SEM (n=6).

Supplementary data

Table S1. Intact glycan analysis of IgG1 Fc-µtp with and without L309C and compared to monomeric IgG1 Fc-µtp C575S.

	IgG1 Fc-µtp L309C	IgG1 Fc-µtp	IgG1 Fc-µtp C575S
Occupancy (%)	68	63	67

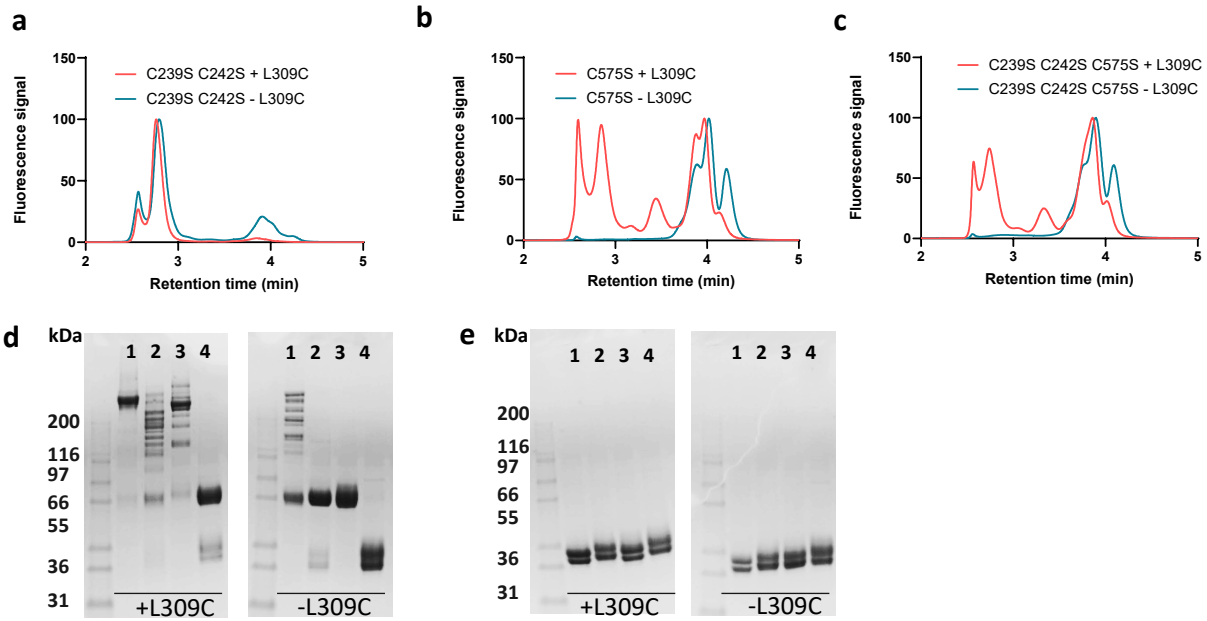


Figure S2. Cys mutations were introduced to IgG1 Fc-µtp and IgG1 Fc-µtp L309C, expressed in CHO-ISXE cells, affinity purified and analysed for its SEC profile in-solution. (A) Analytical SE-UPLC of IgG1 Fc-µtp with L309C (red line) and without L309C (black line) in the presence of hinge mutations C239S C242S **(B)** SE-UPLC of IgG1 Fc-µtp with L309C (red line) and without L309C (black line) in the presence of tp mutation C575S **(C)** SE-UPLC of IgG1 Fc-µtp with L309C (red line) and without L309C (black line) in the presence of hinge and tp mutations C239S C242S C575S. SDS-PAGE analysis of IgG1 Fc-µtp fusion molecules with and without L309C under non-reducing **(D)** and reducing **(E)** conditions.

Supplementary data

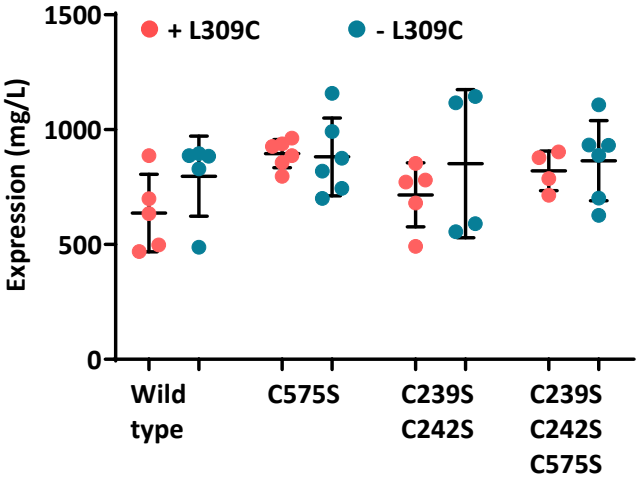


Figure S3. Expression analysis of IgG1-Fc µtp with and without L309C. Cys mutations were introduced to the hinge (C239S C242S) or tp (C575S), or to both regions (C239S C242S C575S). Each data point represents a single transfection. IgG1 Fc-µtp L309C is represented by black dots (●) and IgG1 Fc-µtp is represented by red dots (●). At least four transfections were performed per construct and data shows no difference in expression between variants.

Supplementary data

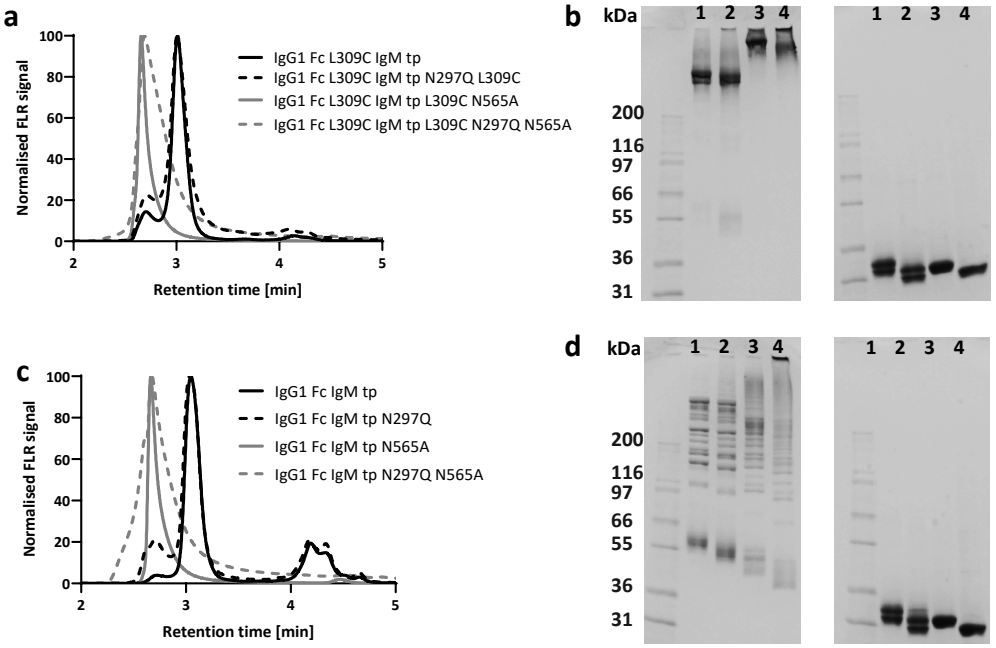


Figure S4. SE-UPLC and SDS-PAGE analyses of N-linked glycan mutants of IgG1-µtp fusions expressed with (**A and B**) and without (**C and D**) L309C. No additional mutations represented by solid black chromatogram trace and lane 1. IgG1-µtp N297Q (in Cγ2) represented by the dotted black chromatogram trace and lane 2. IgG1-µtp N563A represented by solid grey chromatogram trace and lane 3 Lane 4: IgG1-µtp N297Q (in Cγ2). IgG1-µtp N297Q and N563A represented by the dotted grey chromatogram trace and lane 4.

Supplementary data

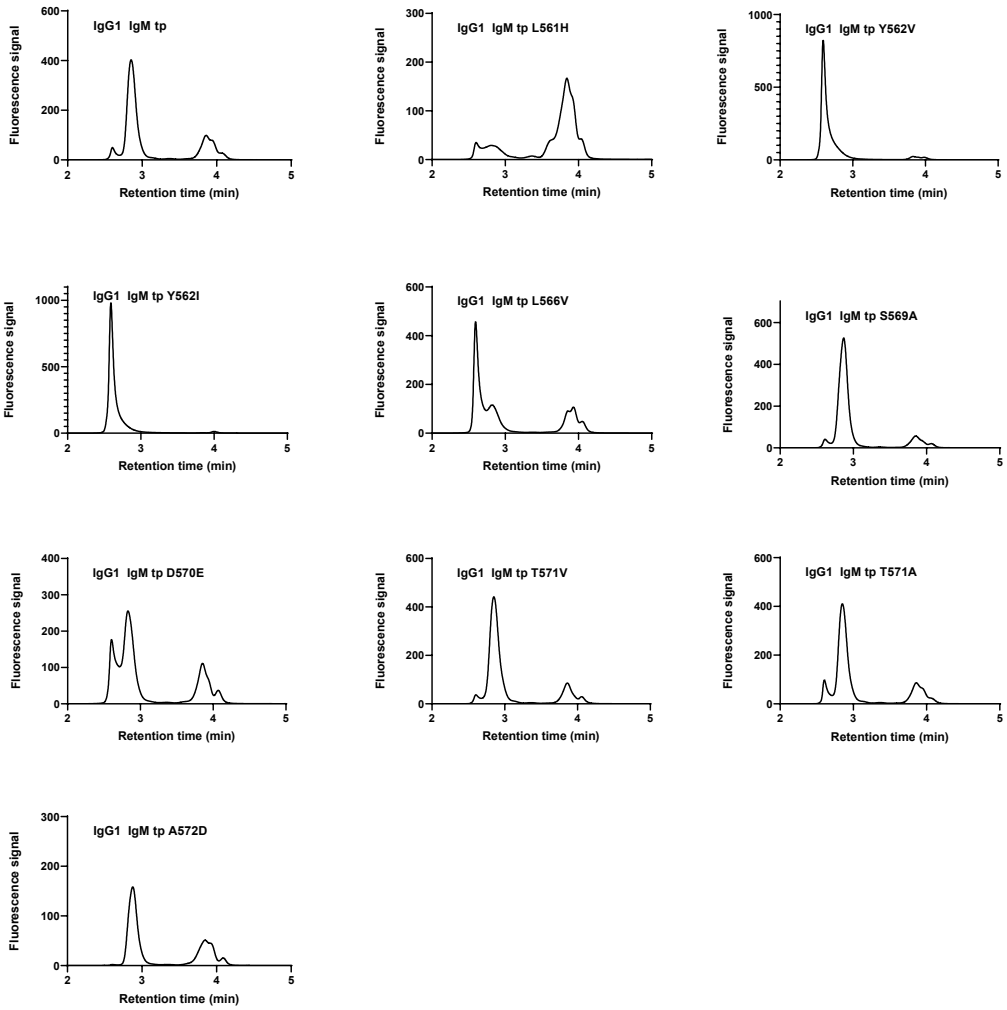


Figure S5. SE-UPLC analysis of IgG1 Fc-αtp mutants. αtp residues were introduced to µtp fusion molecules. Hexamerisation is decreased for L561, Y562, L566 and to a lesser degree, D570. N=2, traces representative of one experiment.

Supplementary data

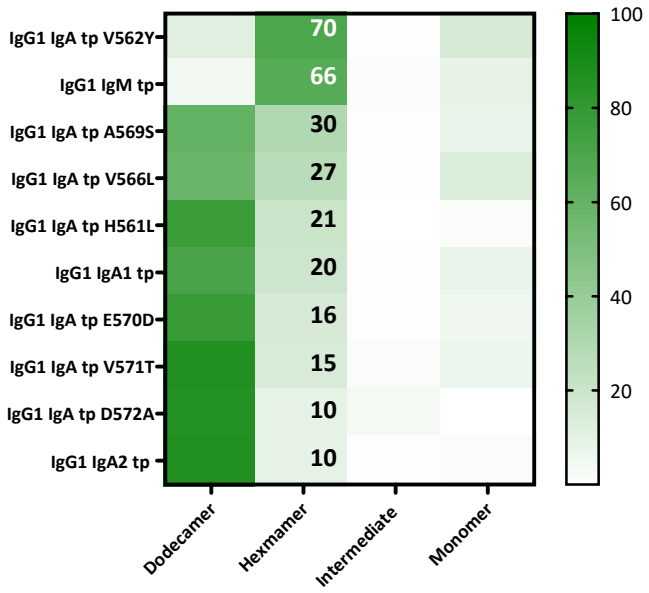


Figure S6. Human IgG1 Fc was fused to tp sequences from human α1tp or α2tp , and variants of αtp towards µtp residues. Molecules were expressed in CHO-SXE cells, affinity purified and subjected to analytical SE-UPLC. Heatmap of SE-UPLC analysis is presented in a heatmap ranked from top to bottom of molecules with highest to lowest percentage hexamer in-solution. Percentage hexamer was determined by peak integration and calculating area under the curve as a percentage of the whole surface area. N=1

Supplementary data

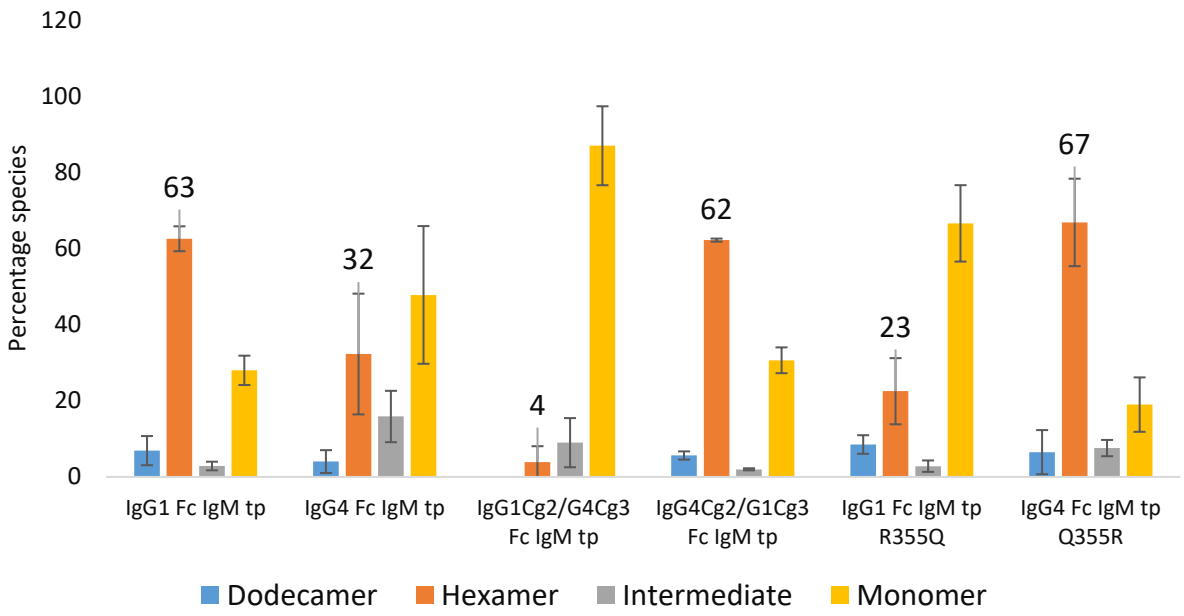


Figure S7. IgG1 Fc-µtp, IgG4 Fc-µtp and constant domain hybrids were expressed from CHO-SXE cells. Affinity purified material was subjected to SE-UPLC analysis to determine percentage hexamer (and other species) expressed from the cell post affinity purification. Percentage hexamer was determined by peak integration and calculating area under the curve as a percentage of the whole surface area. N=3 with technical duplicates within each experiment.

Supplementary data

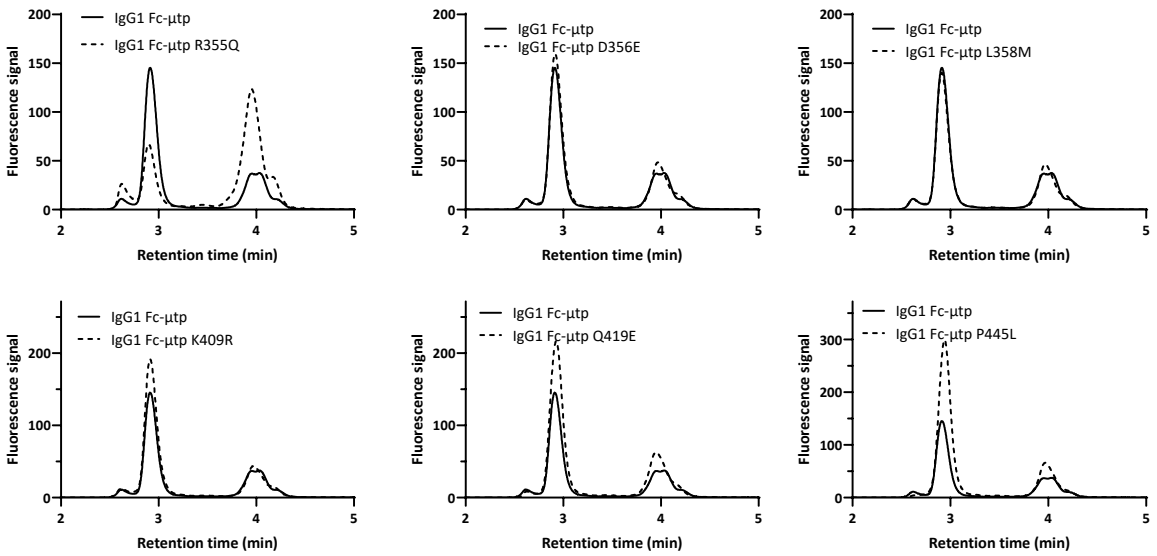


Figure S8. Representative SE-UPLC traces of IgG1 Fc-µtp compared to IgG1 Fc-µtp mutated to every IgG4 Cγ3 residue. Human IgG1 or IgG4 Fc with various mutations were fused to the µtp, expressed in CHO-SXE cells, affinity purified and subjected to analytical SE-UPLC. N=1 with technical replicates

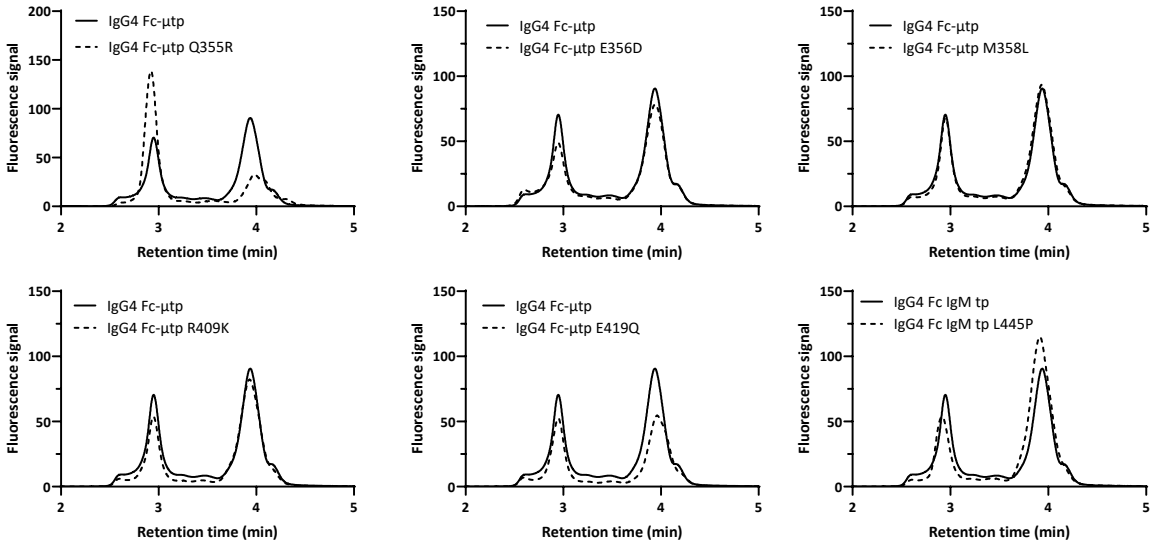


Figure S9. Representative SE-UPLC traces of IgG4 Fc-µtp compared to IgG4 Fc-µtp mutated to every IgG1 Cγ3 residue. Human IgG1 or IgG4 Fc with various mutations were fused to the µtp, expressed in CHO-SXE cells, affinity purified and subjected to analytical SE-UPLC. N=1 with technical replicates

Supplementary data

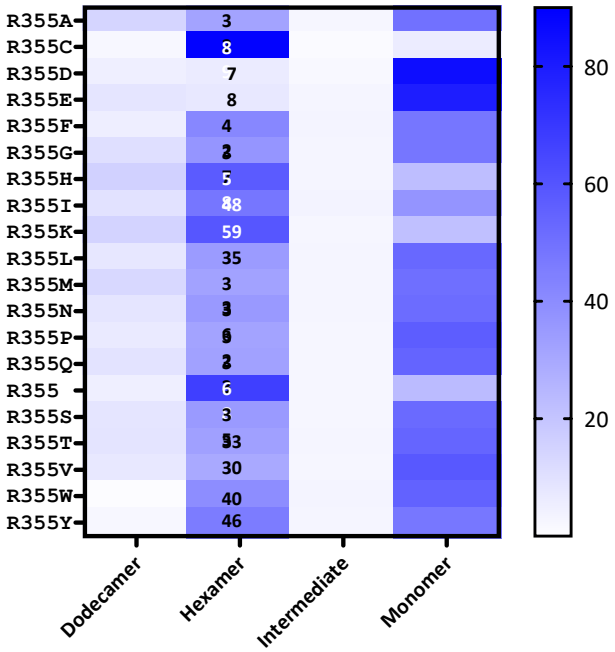


Figure S10. SE-UPLC analysis of IgG1 Fc-µtp variants at position 355. Human IgG1 Fc-µtp with various mutations were expressed in CHO-SXE cells, affinity purified and subjected to analytical SE-UPLC. Percentage hexamer was determined by peak integration and calculating area under the curve as a percentage of the whole surface area. N=1

Supplementary data

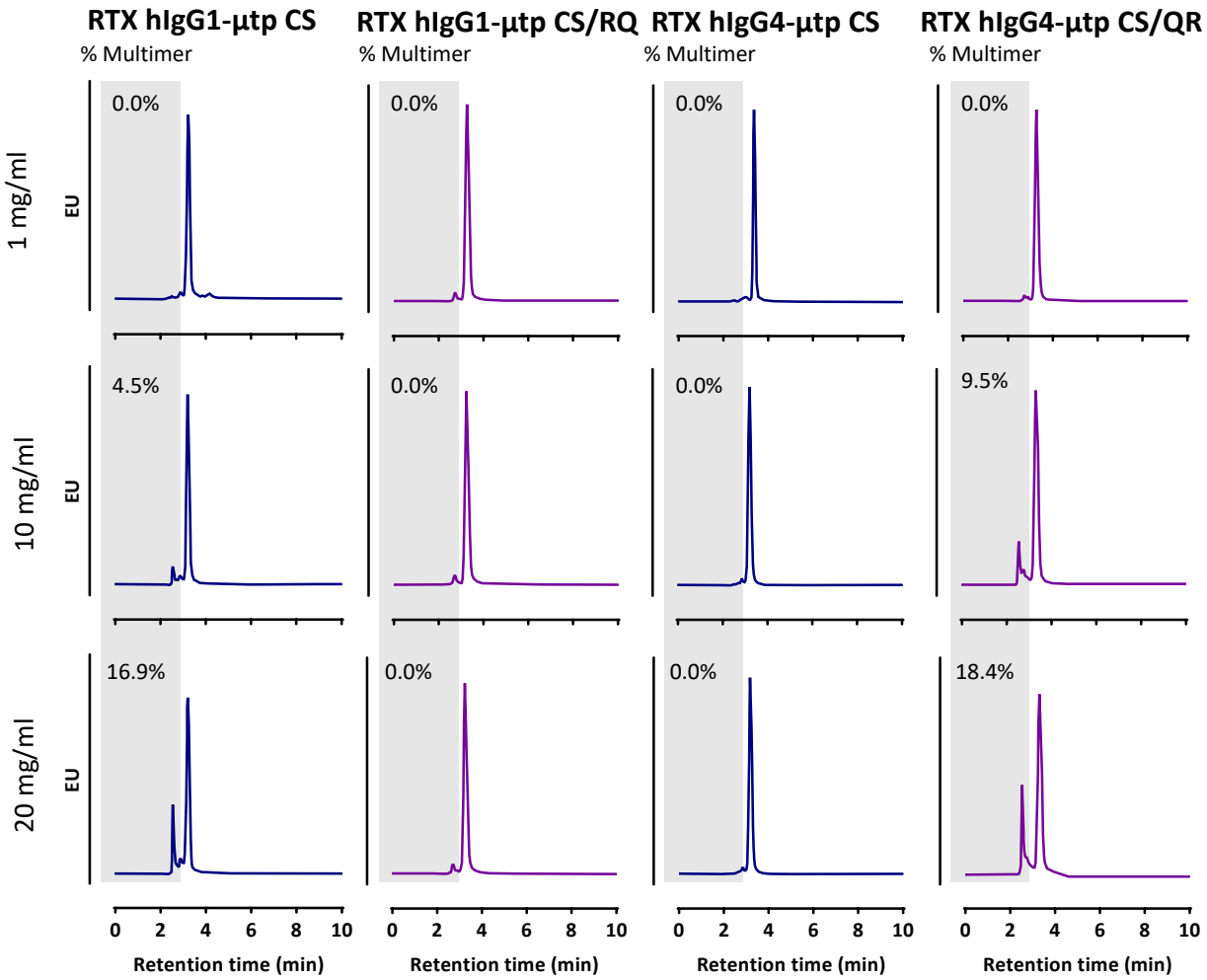


Figure S11. Modification of residue 355 alters the hexamerisation potential of full-length IgG. In-solution hexamerisation was measured by concentrating RTX hIgG1-µtp C575S, -µtp C575S/R355Q and RTX hIgG4-µtp C575S, -µtp C575S/Q355R mAb up to 20 mg/ml and then diluting and analysing by SE-UPLC and the percentage of monomeric and multimeric species calculated by peak integration.

Supplementary data

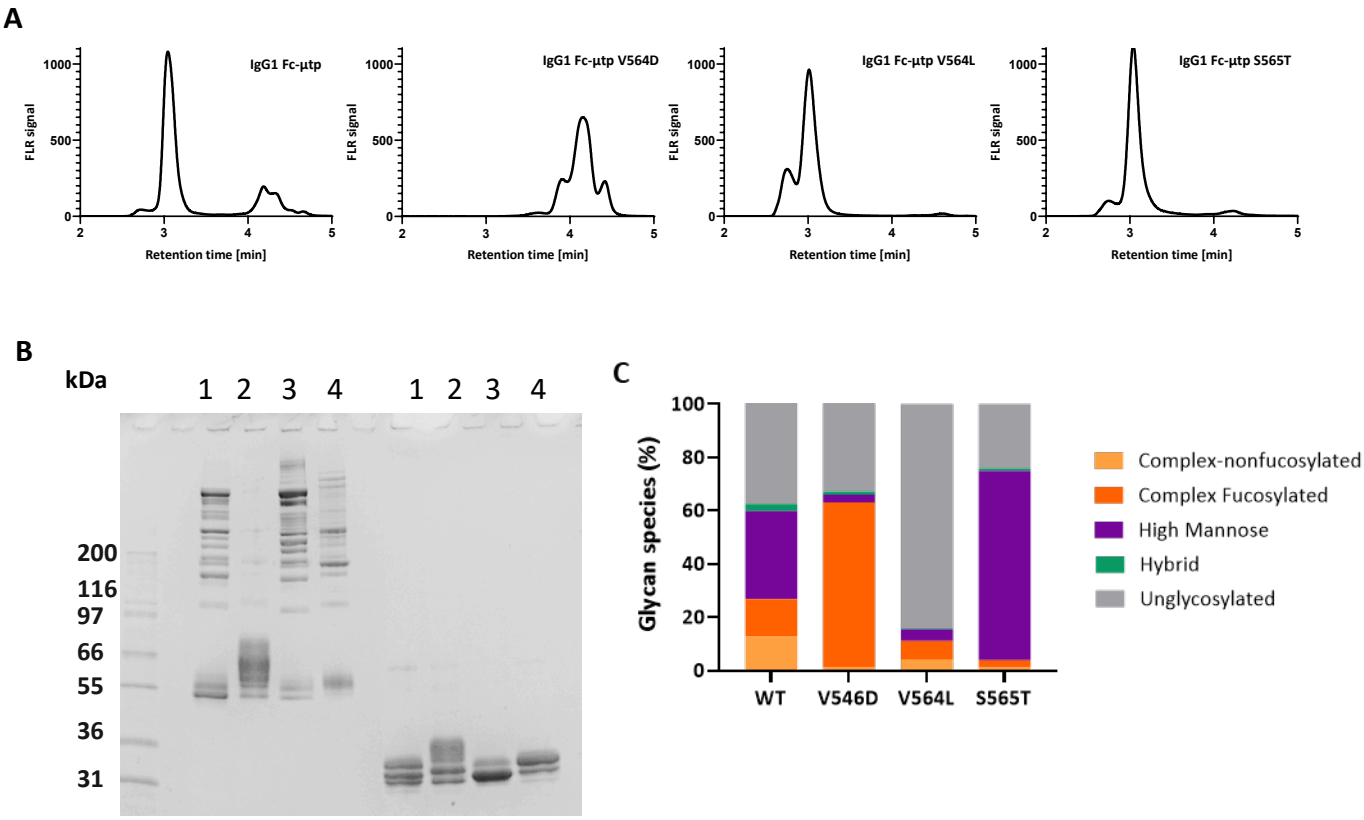


Figure S12. Residue changes to the µtp glycosylation site alter the multimeric state of IgG1 Fc-µtp fusion proteins. **(A)** Analytical size exclusion chromatography of V564 and S565 mutants of IgG1 Fc-µtp. **(B)** SDS-PAGE analysis of samples under non-reducing (left panel) and reducing conditions (right panel). Lanes 1-4 are IgG1 Fc-µtp, IgG1 Fc-µtp V546D, IgG1 Fc-µtp V456L and IgG1 Fc-µtp S565T, respectively. Approximate sizing was performed by comparison to SDS-PAGE protein ladder (Mark12). **(C)** Glycan profile analysis by peptide mapping, shows greater occupancy for the S565T variant associated also with high mannose levels.